Atmos. Chem. Phys. Discuss., doi:10.5194/acp-2016-294, 2016
Manuscript under review for journal Atmos. Chem. Phys.
Published: 6 June 2016

Atmospheric Chemistry and Physics Discussions

Observation of new particle formation and measurement of sulfuric acid, ammonia, amines and highly oxidized molecules using nitrate CI-APi-TOF at a rural site in central Germany

Andreas Kürten[1], Anton Bergen[1], Martin Heinritzi[1], Markus Leiminger[1], Verena Lorenz[1], Felix Piel[1], Mario Simon[1], Robert Sitals[1], Andrea Wagner[1], and Joachim Curtius[1]

[1]Institute for Atmospheric and Environmental Sciences, Goethe University of Frankfurt, Frankfurt am Main, Germany

Correspondence to: Andreas Kürten (kuerten@iau.uni-frankfurt.de)

Abstract

The exact mechanisms for new particle formation (NPF) under different boundary layer conditions are not known yet. One important question is if amines and sulfuric acid lead to efficient NPF in the atmosphere. Furthermore, it is not clear to what extent highly oxidized organic molecules (HOM) are involved in NPF. We conducted field measurements at a rural site in central Germany in the proximity of three larger dairy farms to investigate if there is a connection between NPF and the presence of amines and/or ammonia due to the local emissions from the farms. Comprehensive measurements using a nitrate Chemical Ionization-Atmospheric Pressure interface-Time Of Flight (CI-APi-TOF) mass spectrometer, a Proton Transfer Reaction-Mass Spectrometer (PTR-MS), particle counters and Differential Mobility Analyzers (DMAs) as well as measurements of trace gases and meteorological parameters were performed. It is shown that the nitrate CI-APi-TOF is suitable for sensitive measurements of sulfuric acid, amines, a nitrosamine, ammonia, iodic acid and HOM. NPF was found to correlate with sulfuric acid, while an anti-correlation with RH, amines and ammonia is observed. The anti-correlation between NPF and amines could be due to the efficient uptake of these compounds by nucleating clusters and small particles. Much higher HOM dimer (C19/C20 compounds) concentrations during the night than during the day indicate that these HOM do not efficiently self-nucleate as no night-time NPF is observed. Observed iodic acid probably originates from an iodine-containing reservoir substance but the iodine signals are very likely too low to have a significant effect on NPF.

1. Introduction

Atmos. Chem. Phys. Discuss., doi:10.5194/acp-2016-294, 2016
Manuscript under review for journal Atmos. Chem. Phys.
Published: 6 June 2016

Atmospheric Chemistry and Physics Discussions

The formation of new particles from gaseous compounds (nucleation) produces a larger fraction of atmospheric aerosol particles (Zhang et al., 2012). While the newly formed particles have diameters between 1 and 2 nm they can grow and reach larger sizes, which enables them to act as cloud condensation nuclei (CCN, ~50 nm in diameter or larger). Removal processes such as coagulation scavenging due to larger pre-existing particles can be important if the growth rates (*GR*) for the newly formed particles are slow and/or if the coagulation sink (*CS*) is high. The climatic effect of nucleation depends strongly on the survival probability of the newly formed particles, i.e. if they reach CCN size, or not. Model calculations indicate that nucleation can account for ca. 50% of the CCN population globally (Merikanto et al., 2009). In addition to their climatic effect secondary particles can also influence the human health (Nel, 2005), or reduce visibility, e.g. in megacities (Chang et al., 2009).

New particle formation (NPF) is a global phenomenon and has been observed in many different environments (Kulmala et al., 2004). In most cases a positive correlation with the concentration of gaseous sulfuric acid has been observed (Sihto et al., 2006; Kuang et al., 2008). However, other trace gases, beside H_2SO_4 and H_2O, need to be involved in the formation of clusters, otherwise the high particle formation rates measured in the boundary layer cannot be explained (Weber et al., 1997; Kirkby et al., 2011). One ternary compound, which enhances the binary nucleation of sulfuric acid and water significantly, is ammonia. However, at the relatively warm temperatures of the boundary layer the presence of ammonia is probably not sufficient for reaching the observed NPF rates when acting together with sulfuric acid and water (Kirkby et al., 2011; Kürten et al., 2016). The same applies for ion-induced nucleation (IIN); the observed IIN rates for the binary and ternary system including ammonia are not high enough to explain the observations (Kirkby et al., 2011). Therefore, recent nucleation experiments focused on organic compounds acting as a ternary compound (beside H_2SO_4 and H_2O). Many studies indicate that amines have a very strong enhancing effect on nucleation (Kurtén et al., 2008; Chen et al., 2012; Glasoe et al., 2015). Indeed, a chamber experiment could show that the nucleation of sulfuric acid, water and dimethylamine (DMA) at 5°C and 38% RH produced particles at a rate, which is compatible with atmospheric observations in the boundary layer over a relatively wide range of sulfuric acid concentrations (Almeida et al., 2013). For sulfuric acid concentrations $<10^7$ molecule cm^{-3}, which are typical for the boundary layer, and dimethylamine mixing ratios of > ~10 pptv, nucleation was found to proceed at or close to the kinetic limit. This means every collision between sulfuric acid molecules, and clusters associated with DMA, leads to a larger cluster, which does not evaporate significantly (Kürten et al., 2014).

In principle, mass spectrometry using nitrate chemical ionization could be used to detect neutral clusters consisting of sulfuric acid and bases in the atmosphere. However, only few studies indicate that neutral nucleating atmospheric clusters consist of sulfuric acid and ammonia or amines (Zhao et al., 2011; Jiang et al., 2011), while other studies could not identify such clusters (Jokinen et al., 2012; Sarnela et al., 2015). A further outstanding issue is the question about the magnitude of the atmospheric amine mixing ratios at different locations. In the past several years the experimental tools for sensitive

Atmos. Chem. Phys. Discuss., doi:10.5194/acp-2016-294, 2016
Manuscript under review for journal Atmos. Chem. Phys.
Published: 6 June 2016

online measurement of amines in the pptv-range became available (Hanson et al., 2011; Yu and Lee 2012). The reported amine levels reach from up to tens of pptv (Hanson et al., 2011; Freshour et al., 2014; You et al., 2014; Hellén et al., 2014) to < 0.1 pptv (Sipilä et al., 2015). It is therefore an important question if some of the reported mixing ratios could be biased high or low due to instrumental issues, or if the natural variability in the amine mixing ratios due to different source strengths can explain the differences.

Other possible contributors to particle formation are highly oxidized organic compounds originating e.g. from the reaction of monoterpenes with atmospheric oxidants (Zhao et al., 2013; Ehn et al., 2014; Riccobono et al., 2014; Jokinen et al., 2015; Kirkby et al., 2016). From this perspective it seems likely that different nucleation pathways are possible and may dominate at different sites depending, e.g. on the concentration of sulfuric acid, amines, oxidized organic compounds and other parameters like temperature and relative humidity. Synergistic effects are also possible, e.g. it has been demonstrated that the combined effect of ammonia and amines can lead to more efficient particle formation with sulfuric acid and water than for a case where ammonia is not present (Glasoe et al., 2015). Due to the manifold possibilities for nucleation and the low concentrations of the growing clusters it is challenging to identify the dominating particle formation pathway from field measurements in an environment where many possible ingredients for nucleation are present at the same time. However, such measurements are necessary and previous measurements from Hyytiälä, Finland, underscored the importance of sulfuric acid, organic compounds and amines regarding NPF (Kulmala et al., 2013).

In this study, we have chosen to conduct measurements with an emphasis on the observation of NPF at a rural site in central Germany. The goal of this field campaign was to measure NPF in an amine rich environment in the vicinity of dairy farms, as cows are known to emit a variety of different amines as well as ammonia (Schade and Crutzen, 1995; Ge and Wexler, 2011; Sintermann et al., 2014). The measurements were performed using different particle counters and particle size analyzers as well as trace gas monitors (O_3, SO_2 and NO_x). A Proton Transfer Reaction-Mass Spectrometer (PTR-MS) is used to determine the gas-phase concentration of monoterpenes and isoprene, whereas a chemical ionization time of flight mass spectrometer using nitrate primary ions (Jokinen et al., 2012; Kürten et al., 2014) is used for the measurement of sulfuric acid, amines, ammonia and highly oxidized organics.

2. Methods and Measurement Site Description

2.1 Measurement Site Description

The measurement site is located right next to a meteorological weather station operated by the German Weather Service (DWD measurement station Michelstadt-Vielbrunn/Odenwald, 49°43'04.4" N and 09°05'58.9" E, 452 m a.s.l.). The village Vielbrunn has a total of ~1300 inhabitants and is surrounded

Atmos. Chem. Phys. Discuss., doi:10.5194/acp-2016-294, 2016
Manuscript under review for journal Atmos. Chem. Phys.
Published: 6 June 2016

by fields and forests. The next larger cities are Darmstadt (~35 km towards WNW) and Frankfurt/Main (~50 km towards NNW). The site was chosen for several reasons: (i) three larger dairy farms are close by, which should possibly enable us to study the effect of amines on new particle formation, (ii) it can be regarded as typical for a rural or agricultural area in central Europe, (iii) the site is not too far away from the University of Frankfurt, which allows to visit the station for instrument maintenance on a daily basis and (iv) since we could measure right next to a meteorological station infrastructure and meteorological data from the DWD could be used.

In terms of studying the effect of amines on new particle formation we were expecting to see a direct effect due to the local emissions from the dairy farms. Each of these farms is keeping a couple of hundred cows in shelters, which are essentially consisting only of a roof and a fence such that the wind can easily carry away the emissions. As mentioned in the introduction livestock is known to emit a variety of amines as well as ammonia (Schade and Crutzen, 1995; Sintermann et al. 2014) both of which should have an influence on new particle formation and growth (Almeida et al., 2013; Lehtipalo et al., 2016). The farms are located in the West (~ 450 m distance), South-South-West (~ 1100 m distance) and South-East (~ 750 m distance) of the station, respectively.

One further aspect that should be considered is the fact that the site is also surrounded by forests (mixed type of coniferous and deciduous trees, at least 1 km away). Consequently, emissions of, e.g. monoterpenes ($C_{10}H_{16}$ compounds), can also potentially influence new particle formation as recent studies indicate that their oxidation products can contribute to NPF and particle growth (Schobesberger et al., 2013; Riccobono et al., 2014; Ehn et al., 2014; Kirkby et al., 2016).

2.2 CI-APi-TOF

The key instrument for the data discussed in this study is the Chemical Ionization-Atmospheric Pressure interface-Time Of Flight mass spectrometer (CI-APi-TOF). The instrument was first introduced by Jokinen et al. (2012) and the one used in the present study is described by Kürten et al. (2014). The CI-APi-TOF draws a sample flow of 8.5 slm (standard liters per minute), which interacts with nitrate primary ions ($(HNO_3)_{0-2}\ NO_3^-$) within an ion reaction zone at ambient pressure (~ 50 ms reaction time). The primary ions are generated from the interaction of HNO_3 in a sheath gas and a negative corona discharge (Kürten et al., 2011). The ion source is based on the design by Eisele and Tanner (1993) for the measurement of sulfuric acid. The primary and product ions are drawn into the first stage of a vacuum chamber through a pinhole (~350 µm diameter). Quadrupoles in the first and a second stage of the chamber, operated in rf-only mode, are used to guide the ions. A lens stack in a third stage focuses and prepares the ions energetically before they enter the time of flight mass spectrometer (Aerodyne Research Inc., USA and Tofwerk AG, Switzerland). This mass spectrometer has a mass resolving power of ~4000 Th/Th and a mass accuracy of better than 10 ppm. These characteristics allow the elemental identification of unknown ions, i.e. different species having the same nominal (integer) *m*/*z* ratio can be

Atmos. Chem. Phys. Discuss., doi:10.5194/acp-2016-294, 2016
Manuscript under review for journal Atmos. Chem. Phys.
Published: 6 June 2016

Atmospheric Chemistry and Physics Discussions

separated due to their mass defect. Using isotopic patterns for an expected ion composition supports the ion identification. For the data analysis the software tofTools (Junninen et al., 2010) is used within the Matlab environment.

Previous work has shown that the CI-APi-TOF can be used for highly sensitive measurements of sulfuric acid (Jokinen et al., 2012), clusters of sulfuric acid and dimethylamine (Kürten et al., 2014), organic compounds with very low volatility (Ehn et al., 2014) and dimethylamine (Simon et al., 2016). Sulfuric acid and its clusters can be detected after donating a proton to the primary ions, whereas the low volatility organic compounds are detected after clustering with NO_3^-. The measurement of amines is possible because they can be associated with nitrate cluster ions (Section 3.6). Generally, the quantification of a substance is derived with the following equation:

$$concentration = C \cdot ln\left(1 + \frac{\sum product\ ion\ count\ rates}{\sum primary\ ion\ count\ rates}\right). \quad (1)$$

Equation (1) relates the sum of the product ion count rates to the sum of the primary ion count rates. Using a calibration constant *C* the concentration of a neutral substance can be determined. In the case of the sulfuric acid concentration ($[H_2SO_4]$) the product ion count rates are due to HSO_4^- and $(HNO_3)HSO_4^-$, while the primary ion count rates include NO_3^-, $(HNO_3)NO_3^-$ and $(HNO_3)_2NO_3^-$. The calibration constant has been determined as 6×10^9 molecule cm^{-3} (Kürten et al., 2012).

The same calibration constant has also been used for the quantification of HOM. However, in this case the mass dependent transmission of the CI-APi-TOF was taken into account by the method of Heinritzi et al. (2016). This requires an additional correction factor in equation (1) which is around 0.4 for the *m*/*z* range 300 to 400 Th and 0.22 for the range 500 to 650 Th; these factors take into account only the transmission as function of the *m*/*z* value, while assuming the same ionization efficiency as for sulfuric acid, which has been argued to be a valid assumption (Ehn et al., 2014). The quantification of amines will be detailed in Section 3.6. Table 1 gives an overview of the identified ion signals used in the further analysis evaluating sulfuric acid monomer and dimer concentrations as well as amine, nitrosamine, ammonia and iodic acid signals (further explanations will be given in the following sections).

Regarding the loss of sample molecules within the inlet line of the CI-APi-TOF we expect only a minor effect. As the sample line has a total length around 1 m, a very high flow rate was applied over most of the inlet length (Berresheim et al., 2000). Only for the last ~15 cm the flow of 8.5 slm was applied taking the sample from the center part of the first inlet stage where the inlet has a significantly larger diameter (5 cm instead of 1 cm for the last part) to avoid wall contact of the relevant portion of the sampled air.

2.3 PTR-MS

Atmos. Chem. Phys. Discuss., doi:10.5194/acp-2016-294, 2016
Manuscript under review for journal Atmos. Chem. Phys.
Published: 6 June 2016

Atmospheric Chemistry and Physics Discussions

Volatile Organic Compounds (VOCs) were measured with a calibrated Proton Transfer Reaction-Mass Spectrometer (PTR-MS using a quadrupole mass spectrometer, IONICON GmbH, Innsbruck, Austria). The instrument inlet was heated to 60°C and the same temperature was applied to the ion drift tube. The drift tube was operated at an *E*/*N* of 126 Td in order to minimize the formation of protonated water clusters while maintaining a high sensitivity (*E*/*N* is the ratio between the electric field strength *E* in V cm^{-1} and the number density *N* of gas molecules in cm^{-3}, see Blake et al., 2009).

A calibration of the instrument was performed prior to the campaign with a gas mixture containing several VOCs at a known volume mixing ratio (Ionimed-VOC-Standard, Innsbruck, Austria), including isoprene, α-pinene, and acetone amongst others. The calibration was performed for a relative humidity range of 0 to 100 % (steps of 20 %) at room temperature. However, especially for α-pinene (measured at 81 and 137 Th), the sensitivity of the PTR-MS operating at the rather high *E*/*N* was not depending on relative humidity. For isoprene (measured at 41 and 69 Th), a higher RH led to lower fragmentation inside the instrument, but this did not affect the overall sensitivity much (<5 % decrease from 20 to 100%).

The PTR-MS cannot readily distinguish between different monoterpenes as all have the same molecular weight, so only the sum of monoterpenes could be measured. However, since α-pinene is often the most abundant monoterpene in continental mid latitudes (Geron et al., 2000; Janson and de Serves, 2001) and the reaction rate constants for different monoterpenes are rather similar (Tani et al., 2003; Cappellin et al., 2012) our estimation of total monoterpene concentration should not be affected by large errors.

2.4 Other instrumentation

Trace gas monitors were used to measure the mixing ratios of sulfur dioxide (Model 43i TLE Trace Level SO_2 Analyzer, Thermo Scientific), ozone (Model 400, Ozone Monitor, Teledyne API) and nitrogen oxides (NO_x, Ambient NO_x-Monitor APNA-360, Horiba). These instruments were calibrated once before the campaign with known amounts of trace gases and dry zero air was applied on a daily basis for a duration of at least half an hour in order to take instrument drifts into account.

Further instruments used include condensation particle counters (CPCs) and differential mobility analyzers (DMAs). The CPCs 3025A and 3010 (TSI, Inc.) were used to determine the total particle concentration above their cut-off sizes of 2.5 and 10 nm, respectively. A Scanning Mobility Particle Sizer (SMPS) from TSI (Model 3081 long DMA with a CPC 3776) determined the particle size distribution between 16 and 600 nm. The smaller size range was covered by a nDMA (Grimm Aerosol Technik, Germany) and a TSI CPC 3776 for diameters between 3 and 40 nm. The combined size distribution can be used to calculate the condensation/coagulation sink towards certain trace gases (e.g. sulfuric acid) or particle diameters.

Atmos. Chem. Phys. Discuss., doi:10.5194/acp-2016-294, 2016
Manuscript under review for journal Atmos. Chem. Phys.
Published: 6 June 2016

Meteorological parameters were both obtained from our own measurements with a Vaisala sonde (Model WXT 520), which yielded the temperature, RH, wind speed and direction as well as the amount of precipitation. The same parameters are also available for the Vielbrunn meteorological station from the DWD; additionally, values for the global radiation were provided from the DWD.

3. Results

3.1 Meteorological conditions and overview

The intensive phase of the campaign was from May 18 to June 7, 2014 (21 campaign days). Figure 1 shows an overview of the meteorological conditions, i.e. temperature, relative humidity, global radiation and precipitation. The size distribution of small particles (Fig. 1, bottom panel) was measured by the nDMA. In addition, the condensation sink calculated for the loss of sulfuric acid on aerosol particles is also shown taking into account the full size distribution (up to 600 nm).

The first part of the campaign (including May 22) was characterized by warm temperatures and sunny weather without precipitation. Between May 22/23 and May 31 the weather conditions were less stable with colder temperatures and some precipitation events. Especially on May 29 a strong drop in temperature and the condensation sink was observed, due to a cold front followed by the passage of relatively clean air. From May 31 on temperatures were increasing again and it was mostly sunny with only two rain events on June 3 and June 4.

Elevated concentrations of small particles could be observed on almost every day. However, new particle formation from the smallest sizes (around 3 nm) followed by clear growth were seen only on 6 days out of 21 (i.e. 29%). These events, which were also used for the calculation of new particle formation rates (Section 3.9), are highlighted in the bottom panel of Fig. 1 by the dark gray arrows. The presence of small particles was also observed on several other days, however, the events were either relatively weak, or no clear particle growth was observable.

3.2 Trace gas measurements

The trace gas measurements are shown in Fig. 2. Typical maximum day-time ozone mixing ratios ranged from ~40 to 75 ppbv (Fig. 2, upper panel). The sulfur dioxide levels were between 0.05 and a maximum of 2 ppbv with average values around 0.3 ppbv (Fig. 2, upper panel). Especially during the passage of clean air on May 29 and May 30 the SO_2 levels were quite low. NO_2 mixing ratios showed a distinct diurnal pattern with a minimum in the late afternoon and an average mixing ratio around 3 ppbv (Fig. 2, middle panel, see also Fig. 8). The NO mixing ratios were about a factor of 5 lower compared to NO_2 on average (Fig. 2, middle panel, see also Fig. 8); similar values were reported for another rural site in

Atmos. Chem. Phys. Discuss., doi:10.5194/acp-2016-294, 2016
Manuscript under review for journal Atmos. Chem. Phys.
Published: 6 June 2016

Germany (Mutzel et al., 2015). The maximum sulfuric acid concentrations were reached around noon and ranged between ~1×10^6 and 2×10^7 molecule cm^{-3} (Fig. 2, lower panel, see also Fig. 3), which is comparable to other sites (Fiedler et al., 2005; Petäjä et al., 2009). The total monoterpene and isoprene mixing ratios measured by the PTR-MS were similar to each other with values between ~0.03 and 1 ppbv (Fig. 2, lower panel). Mixing ratios in the same range have also been reported for the boreal forest (Rantala et al., 2014).

3.3 H_2SO_4 measurement and calculation from proxies

Figure 3 shows the average diurnal sulfuric acid concentration along with other data, which will be discussed in later sections. The maximum average [H_2SO_4] around noon was ~3×10^6 molecule cm^{-3}; the error bars represent one standard deviation.

Recently, Mikkonen et al. (2011) introduced approximations to calculate sulfuric acid as a function of different proxies. Since the relevant parameters (sulfur dioxide mixing ratio, global radiation, relative humidity and condensation sink) are available, we have used the following formula to approximate the sulfuric acid concentration (Mikkonen et al., 2011):

$$[\mathrm{H_2SO_4}]_{proxy} = a \cdot k(T,p) \cdot [\mathrm{SO_2}]^b \cdot Rad^c \cdot RH^d \cdot CS^e. \quad (2)$$

The [H_2SO_4] (expressed in molecule cm^{-3}) is calculated as a function of the SO_2 mixing ratio (in ppbv), the global radiation *Rad* (in W m^{-2}), the relative humidity *RH* (in %), the condensation sink *CS* (in s^{-1}), a rate constant *k*, which depends on ambient pressure *p* and temperature *T* (see definition for *k* by Mikkonen et al., 2011) and a scaling factor *a*. A least square fit made with the software IGOR yields the coefficients $a = 1.321\times10^{15}$, $b = 0.913$, $c = 0.990$, $d = -0.217$ and $e = -0.526$ (linear correlation coefficient, Pearson's *r*, is 0.87). Following the recommendations given by Mikkonen et al. (2011) we restricted the data used in the derivation of the parameters to conditions where the global radiation was equal or larger than 50 W m^{-2}. In addition, a simpler formulation was also tested, which neglects the dependence on *RH* and *CS*:

$$[\mathrm{H_2SO_4}]_{proxy'} = a' \cdot k(T,p) \cdot [\mathrm{SO_2}]^{b'} \cdot Rad^{c'}. \quad (3)$$

Here, the coefficients $a' = 1.343\times10^{16}$, $b' = 0.786$ and $c' = 0.941$ yield good agreement (linear correlation coefficient, Pearson's *r*, is 0.85) between calculated and measured [H_2SO_4]. Figure 4 shows a comparison between the two approximation methods and the measured sulfuric acid for the full campaign (when $Rad \geq 50$ W m^{-2}). In almost all cases the predicted 5 minute averages are within a factor of 3 of the measured values for both methods. This indicates that even the simpler method (equation (3)) yields relatively accurate results for the conditions of this study. This can probably be

Atmos. Chem. Phys. Discuss., doi:10.5194/acp-2016-294, 2016
Manuscript under review for journal Atmos. Chem. Phys.
Published: 6 June 2016

Atmospheric Chemistry and Physics Discussions

explained by the fact that *RH* and *CS* show only relatively small variations over the duration of the campaign and it is therefore not absolutely necessary to include these factors in the sulfuric acid calculation; for longer periods with larger variations it might, however, be beneficial to include *RH* and *CS*. The parameters found are in good agreement with the ones reported by Mikkonen et al. (2011) for different sites.

3.4 Calculated OH

For further data evaluation knowledge of the OH concentrations is useful. Since there was no direct measurement of the hydroxyl radical available, only an estimation based on other measured parameters can be made. This estimation is based on the assumption that most of the sulfuric acid is produced from the reaction between SO_2 and OH. Using the condensation sink *CS* the balance equation between production and loss at steady-state can be used to derive the OH:

$$[OH]_{day} = \frac{CS\cdot[H_2SO_4] - k_{X+SO_2}\cdot[X]\cdot[SO_2]}{k_{OH+SO_2}\cdot[SO_2]} \approx \frac{CS\cdot[H_2SO_4]}{k_{OH+SO_2}\cdot[SO_2]}. \quad (4)$$

Recently it was discovered that there are also other species capable of oxidizing SO_2 to SO_3 (which lead to subsequent production of H_2SO_4 due to further reactions with O_2 and H_2O) (Mauldin et al., 2012). Those species X, e.g. stabilized Criegee Intermediates (sCI) can be formed via the ozonolysis of alkenes (e.g. isoprene, α-pinene, limonene) (Mauldin et al., 2012; Berndt et al., 2014). Therefore, if some H_2SO_4 is generated from sCI reactions with SO_2, then the calculated OH is an upper estimate. During the day this effect should be relatively small, i.e. < 50% (Boy et al., 2013; Sarwar et al., 2013), although Berndt et al. (2014) state that no final answer can be given regarding the effect of the sCI on the sulfuric acid formation because it depends strongly on the sCI structure and competitive reactions between sCI and water vapor. The derived diurnal pattern of [OH] is shown in Fig. 3 with a maximum concentration of 1×10^6 molecule cm^{-3} around noon, which is in good agreement with other studies (Berresheim et al., 2000; Rohrer and Berresheim, 2006; Petäjä et al., 2009). The calculated OH concentrations were used in Sections 3.5 and 3.8.

3.5 Iodic acid (HIO_3) and OIO

The high resolution CI-APi-TOF mass spectra revealed the presence of iodine containing substances. It can be ruled out that these signals result from instrument contamination as our CI-APi-TOF had never been in contact with iodine (i.e. no nucleation experiments with iodine have yet been performed and no iodide primary ions have been used). The observed signals could be assigned to IO_3^-, $(H_2O)IO_3^-$and $(HNO_3)IO_3^-$ (Table 1). To our knowledge the identification of iodine related peaks have not been

Atmos. Chem. Phys. Discuss., doi:10.5194/acp-2016-294, 2016
Manuscript under review for journal Atmos. Chem. Phys.
Published: 6 June 2016

Atmospheric Chemistry and Physics Discussions

reported from measurements with a nitrate CIMS. However, Berresheim et al. (2000) reported the presence of a peak at *m*/*z* 175 in the spectrum for the marine environment, which was not identified previously but in the light of this study, can almost certainly be attributed to IO_3^-.

The diurnal pattern of IO_3^- and the related iodine peaks show a distinct pattern with a maximum around noon following almost perfectly the diurnal pattern of sulfuric acid (Fig. 3). This may not be surprising since the formation of HIO_3 is due to reaction between OIO and OH (Saiz-Lopez et al., 2012); therefore the iodic acid concentration is connected to the OH chemistry. After normalization of the iodic acid signals with the nitrate primary ion count rates, a concentration of the neutral compound HIO_3 can be obtained by tentatively adopting the same calibration constant for iodic acid than for sulfuric acid. Thereby a maximum average day-time concentration of ~3×10^5 molecule cm^{-3} can be found. Further using the derived OH concentrations from the H_2SO_4 and *CS* measurements (Section 3.4) the derived [HIO_3] can be used to further estimate the concentration of OIO (Saiz-Lopez et al, 2012):

$$[\mathrm{OIO}] = \frac{CS\cdot[\mathrm{HIO_3}]}{k_{\mathrm{OH+OIO}}\cdot[\mathrm{OH}]}. \quad (5)$$

Equation (5) assumes that the only production channel of HIO_3 is the reaction between OH and OIO and the only loss mechanism of HIO_3 is the uptake on aerosol. The reaction rate k_{OH+OIO} can be taken from the literature (Plane et al., 2006). In this way the concentration of OIO can be estimated to a typical value of 5×10^6 molecule cm^{-3}, which is much lower than the values reported for the marine environment (3 to 27 pptv, i.e. 7.5×10^7 to 6.8×10^8 molecule cm^{-3}, see Saiz-Lopez et al., 2012).

The relatively low values of [HIO_3] and [OIO] probably indicate that iodine chemistry is not very important in terms of new particle formation at this site. This is supported by the fact that we could not observe any clusters containing e.g. sulfuric acid and iodic acid or clusters containing more than one iodine molecule. However, it is surprising that iodine can be detected more than 400 km away from the nearest coast line. On the other hand, HYSPLIT back trajectory calculations (Stein et al., 2015) reveal that in most cases the air was arriving from westerly directions and therefore had contact with the ocean within the last 48 hours before arriving at the station. During the measurement period there was unfortunately never a day where the air was clearly coming from easterly directions and had not been in contact with the Atlantic Ocean or Mediterranean Sea within the previous days. Therefore, it could not be checked if this would result in lower iodine signals. Despite the marine origin of the air masses observed it is not clear how the iodine is transported over relatively large distances without being lost on aerosol particles. If iodic acid is irreversibly lost on aerosol (similar to sulfuric acid) its lifetime should only be on the order of several minutes at typical boundary layer conditions. Therefore, the presence of iodine indicates either a local iodine source, or its transport from marine environments in the form of a reservoir substance, e.g. CH_3I (the lifetime of CH_3I is in the order of 1 week, see Saiz-Lopez et al., 2015), and subsequent release due to photolysis.

Atmos. Chem. Phys. Discuss., doi:10.5194/acp-2016-294, 2016
Manuscript under review for journal Atmos. Chem. Phys.
Published: 6 June 2016

Atmospheric Chemistry and Physics Discussions

Regarding the sensitivity of the CI-APi-TOF it can be said that iodic acid (and, if present, probably also its clusters) can be detected with high sensitivity due to the high negative mass defect of the iodine atom ($\Delta m \approx$ -0.1 Th). This allows the identification and quantification of iodine containing substances because generally there will not be any overlap with another substance having the same integer mass (mass resolving power of the instrument is ~4000 Th/Th, i.e. at *m*/*z* 175 the peak width at half maximum is ~0.04 Th). The method introduced here should therefore allow high-sensitivity measurement of [HIO_3] and also the estimation of [OIO] with the help of equation (5) in future studies. The lowest detectable concentrations should be around 3×10^4 molecule cm^{-3}, or better, for [HIO_3] and 5×10^5 molecule cm^{-3} for [OIO] when assuming the same calibration constant for HIO_3 than for H_2SO_4 and considering the lowest iodine signal from Fig. 3.

3.6 Amine, nitrosamine and ammonia measurements

The detection of dimethylamine (DMA, $(CH_3)_2NH$) by means of nitrate chemical ionization with a CI-APi-TOF has been described previously (Simon et al., 2016). The clustering between diethylamine (DEA) and nitrate ion clusters has also been reported by Luts et al. (2011). The amines detected in the present study include CH_5N (monomethylamine), C_2H_7N (dimethylamine, DMA or ethylamine, EA), C_3H_9N (trimethylamine, TMA or propylamine, PA), $C_4H_{11}N$ (diethylamine, DEA) and $C_6H_{15}N$ (triethylamine, TEA). All these amines are identified as clusters in the CI-APi-TOF spectra where the amines are associated both with the nitrate dimer ((amine)$(HNO_3)NO_3^-$) and the trimer ((amine)$(HNO_3)_2NO_3^-$).

The high mass resolving power of the CI-APi-TOF allowed the identification of five different amines (C1-, C2-, C3-, C4- and C6-amines, see above). Since the amines are all identified at two different masses each (either with the nitrate dimer or the nitrate trimer) plotting the time series of each pair of signals allows further verification of the amine signals since a different time trend would reveal that another ion would interfer with the amine signal. This was sometimes the case when the relative humidity was high and clusters of water and nitrate appeared with high water numbers. The cluster of NO_3^- and 6 water molecules has a mass of 170.0518 Th and the C2-amine cluster $(C_2H_7N)(HNO_3)NO_3^-$ (170.0419 Th) cannot be separated from this primary ion cluster. Therefore, if large nitrate plus water clusters were observed in the spectra, no C2-amine signal could be evaluated.

The same ion cluster chemistry applies for ammonia, which can also bind with the nitrate cluster ions. Consequently, ammonia is detected as $(NH_3)(HNO_3)NO_3^-$ and $(NH_3)(HNO_3)_2NO_3^-$ (Table 1). To our knowledge the existence of these cluster ions has not been reported previously.

In accordance with Simon et al. (2016) the cluster ion signals have been normalized by the following relationship:

$$\text{amine}_{ncps} = \ln\left(1 + \frac{\{(\text{amine})(HNO_3)NO_3^-\}+\{(\text{amine})(HNO_3)_2NO_3^-\}}{\{(HNO_3)_2NO_3^-\}}\right), \quad (6)$$

Atmos. Chem. Phys. Discuss., doi:10.5194/acp-2016-294, 2016
Manuscript under review for journal Atmos. Chem. Phys.
Published: 6 June 2016

Atmospheric Chemistry and Physics Discussions

where the curly brackets denote the count rates of the different ion clusters and the same formula can be used when "amine" is replaced by NH_3 to obtain the normalized ammonia signal. The normalization with the nitrate trimer has been chosen because we think that this is the dominant nitrate ion cluster the amines (and ammonia) can bind to within the CI-APi-TOF ion reaction zone (Simon et al., 2016). Partial evaporation of one HNO_3 from the resulting amine nitrate cluster within the CI-APi-TOF vacuum chamber leads to the spread of the signal over the related masses separated by 62.9956 Th (HNO_3).

In addition, to the five amines mentioned before, we were able to identify dimethylnitrosamine (NDMA, $(CH_3)_2NNO$) from its clusters $((CH_3)_2NNO)(HNO_3)NO_3^-$ and $((CH_3)_2NNO)(HNO_3)_2NO_3^-$ (Table 1). The signals from NDMA show a clear diurnal pattern on some days, which can be up to about two orders of magnitude higher during the night compared to the day. This is in agreement with the formation mechanism of NDMA via the reaction between DMA and HONO (Pitts et al., 1978; Glasson, 1979; Grosjean, 1991). The lower concentrations during the day can be explained by the photolysis of HONO and NDMA. Since only C2-amines are capable of forming nitrosamines no further nitrosamine could be identified from the mass spectra. Only a rough estimation of the mixing ratio can be provided by using the calibration constant from Simon et al. (2016) which was derived for DMA. Using this calibration constant the maximum mixing ratio of NDMA would be ~100 pptv (or 2.5×10^9 molecule cm^{-3}). However, this value has a high uncertainty because no direct calibration with NDMA was performed.

The average diurnal patterns of the four amines and ammonia are shown in Fig. 5. The data are an average over 21 measurement days and the error bars represent one standard deviation. The temperature profile is shown along with the CI-APi-TOF signals. The C4-, C6-amines and ammonia show a distinct diurnal profile, which follows the temperature profile closely. The temperature-dependent signal intensity could be due to partial re-evaporation of amines from the particulate phase. No correlation with temperature is seen for the C1-, C2- and C3-amines, which could indicate efficient stabilization of these amines in the particulate phase due to acid-base reactions (Kirkby et al., 2011; Almeida et al., 2013).

No direct calibration for amines, NDMA and ammonia was performed during the campaign. Therefore, only a rough estimation of the mixing ratios can be made. Using the calibration curve for DMA by Simon et al. (2016), 1×10^{-4} ncps (normalized counts per second) correspond to ~1 pptv of DMA. With this conversion the average mixing ratios are between about 1 and 5 pptv for the amines. The mixing ratios from this study are in a similar range as those reported from measurements in a southeastern US forest (You et al., 2014) but generally lower as those from three different sites in the US (Freshour et al., 2014).

The ncps for ammonia are lower than for the amines, which should not be the case if the sensitivity towards ammonia and amines would be the same because the ammonia mixing ratios are almost certainly higher than the ones for the amines in this environment. The ammonia mixing ratio can be above several ppbv in rural areas (von Bobrutzki et al., 2010). Therefore, the sensitivity of the nitrate

Atmos. Chem. Phys. Discuss., doi:10.5194/acp-2016-294, 2016
Manuscript under review for journal Atmos. Chem. Phys.
Published: 6 June 2016

CI-APi-TOF towards ammonia seems to be significantly lower than for amines. This is reasonable, since other studies found that acid-base clusters between sulfuric acid (including the bisulfate ion) and amines are much more stable compared to sulfuric acid ammonia clusters (Kirkby et al., 2011; Almeida et al., 2013). Therefore, the acid base clustering between nitric acid (including the nitrate ion) and ammonia or amines could follow a similar rule, which would lead to faster evaporation of the ammonia nitrate clusters. For this reason only the relative signals for ammonia can be used at the moment without providing estimated mixing ratios.

Recently it has been suggested that diamines could play an important role in ambient NPF (Jen et al., 2016); however, we could not identify diamines from the high-resolution mass spectra.

3.7 Sulfuric acid dimer

Occasionally, the CI-APi-TOF sulfuric acid dimer signal was above background levels. The dimer ($(H_2SO_4)HSO_4^-$) was identified from the high resolution spectra on nine campaign days. The measured sulfuric acid dimer concentrations are shown as a function of the sulfuric acid monomer concentrations in Fig. 6. For comparison, CLOUD chamber data from nucleation experiments in the ternary sulfuric acid-water-dimethylamine system are included (red circles in Fig. 6, Kürten et al., 2014). In addition, the lower dashed line shows the expected dimer formation due to ion-induced clustering (IIC) of sulfuric acid monomers in the CI-APi-TOF ion reaction zone (Hanson and Eisele, 2002; Zhao et al., 2010).

The data indicate that the measured dimer concentrations are clearly above the background level set by ion-induced clustering. On the other hand the concentrations are lower than what has been measured in CLOUD for kinetic nucleation in the sulfuric acid-water-dimethylamine system at 5°C and 38% RH (Almeida et al., 2013; Kürten et al., 2014). Clearly, the neutral sulfuric acid dimers were stabilized by a ternary compound, otherwise their concentrations would not have been measurable at these relatively warm conditions because the dimer (without a ternary compound) evaporation rate is quite high ($> 10^5$ s^{-1} at 290 K, Hanson and Lovejoy, 2006; Kürten et al., 2015). On the other hand the ternary stabilizing agent evaporates after charging of the sulfuric acid dimers because no cluster between the sulfuric acid dimer and another compound (besides HNO_3 from the ion source) could be identified. This means that although the dimers contained at least one additional molecule in the neutral state, the ionized dimer will be detected as $(H_2SO_4)HSO_4^-$ (Ortega et al., 2014; Jen et al., 2014), which makes it impossible to identify the stabilizing agent. Only when larger clusters of sulfuric acid are present (trimer and larger) stabilizing agents like ammonia or amines can stay in the cluster after charging with the nitrate ion (Zhao et al., 2011; Kirkby et al., 2011; Ortega et al., 2014; Kürten et al., 2014). Unfortunately, no large sulfuric acid clusters (trimer and larger) were measurable during the campaign, probably because their concentrations were too low. Therefore, only speculations about the stabilizing agent responsible for the high dimer concentrations can be made. It is quite unlikely that ammonia would be the only stabilizing compound for the dimers since previous studies have shown that the relatively high dimer concentration

Atmos. Chem. Phys. Discuss., doi:10.5194/acp-2016-294, 2016
Manuscript under review for journal Atmos. Chem. Phys.
Published: 6 June 2016

Atmospheric Chemistry and Physics Discussions

measured at rather low sulfuric acid monomer concentrations (< 2×10^7 molecule cm^{-3}) cannot be explained by sulfuric acid-ammonia-water nucleation (Hanson and Eisele, 2002; Jen et al., 2014). In addition, efficient clustering between sulfuric acid and iodic acid can probably be ruled out (provided that these compounds would be capable of producing a cluster with a low evaporation rate) as the concentrations of iodic acid are quite low (~ 3×10^5 molecule cm^{-3} at maximum, see Section 3.5). This means that the arrival rate of iodic acid on a sulfuric acid dimer is on the order of 10^{-4} s^{-1} (using a collision rate of 5×10^{-10} cm^3 $molecule^{-1}$ s^{-1}). Due to the high evaporation rate of the pure sulfuric acid dimer no significant dimer stabilization by iodic acid can be expected.

Whether amines are responsible for the dimer formation in the present study cannot be concluded. If they were, the lower dimer concentrations compared to the CLOUD chamber results (Kürten et al., 2014) could be attributed to the higher temperatures in the present study, which result in faster evaporation rates. Another explanation would be the lower amine mixing ratios. In the CLOUD study dimethylamine was present at 10 pptv, or higher. In addition, it cannot be concluded that e.g. the measured C2-amines are all dimethylamine, if a significant fraction of them were, e.g., ethylamine, its stabilizing effect could be significantly lower. This remains somewhat speculative as no data regarding NPF from ethylamine and sulfuric acid was found, however, triethylamine was reported to have a relatively weak effect on nucleation compared to DMA or TMA (Glasoe et al., 2015). Other compounds which are present and have been shown to form new particles are HOM (Schobesberger et al., 2013; Ehn et al., 2014; Riccobono et al., 2014;) although their stabilizing effect on neutral sulfuric acid dimers remains to be elucidated.

Regarding the observations shown in Fig. 6, it should be noted that no ion filter (high voltage electric field in the CI-APi-TOF inlet to remove ambient ions) was used in the present study. This could in principle lead to the detection of ambient ions and clusters, which did not undergo charging in the CI-APi-TOF ion reaction zone. If this were the case, no representative concentrations of the corresponding neutral sulfuric acid dimer would be derived. CLOUD studies reported that charged sulfuric acid monomers (HSO_4^-) and dimers ($(H_2SO_4)HSO_4^-$) could be observed with a different nitrate chemical ionization mass spectrometer (CIMS) under some conditions (Rondo et al., 2014; Kürten et al., 2015). However, for ambient measurements, no significant effect could be observed for sulfuric acid monomers (Rondo et al., 2014). In principle, the sulfuric acid dimer could be more strongly affected by the detection of ambient ions since the neutral dimer concentration is much lower than the sulfuric acid monomer, while the negative ambient ion spectrum can be dominated by the charged sulfuric acid dimer (Eisele et al., 2006). Therefore, we cannot entirely rule out that ambient ions had some effect on the data shown in Fig. 6. However, the ambient ions would need to overcome an electric field before they could enter the ion reaction zone (Kürten et al., 2011; Rondo et al., 2014). In the CIMS and the CI-APi-TOF a negative voltage is used to focus the primary ions to the center of the reaction zone, while the sample line is electrically grounded. This means negative ambient ions would need to overcome a repulsing electric field which acts as a barrier. Light ions will be efficiently deflected due to their high mobility

Atmos. Chem. Phys. Discuss., doi:10.5194/acp-2016-294, 2016
Manuscript under review for journal Atmos. Chem. Phys.
Published: 6 June 2016

Atmospheric Chemistry and Physics Discussions

but heavier ions can in principle penetrate more easily. Consequently, CIMS measurements at the CLOUD chamber showed that the apparent dimer signal measured by the CIMS correlated with large ion clusters (pentamer, i.e. $(H_2SO_4)_4HSO_4^-$ and larger, which underwent subsequent fragmentation) but not with the $(H_2SO_4)HSO_4^-$ signal; the charged clusters were measured simultaneously with an APi-TOF (Junninen et al., 2010; Kürten et al., 2015). The CI-APi-TOF used in this study utilized a higher voltage for the ion focusing compared to the CIMS (ca. -500 V instead of -220 V in the CIMS) and should therefore prevent smaller masses even more efficiently from entering the ion source than in the study by Kürten et al. (2015). In addition, the absence of any trimer signal ($(H_2SO_4)_2HSO_4^-$) in the spectra argues against ambient ion detection. In a previous study by Eisele et al. (2006) ambient ion measurements showed, besides signals for $(H_2SO_4)HSO_4^-$, also signals for $(H_2SO_4)_2HSO_4^-$) which were on average ~50% of the dimer signals. Since the CI-APi-TOF design, with its repulsing voltages towards ambient ions in the ion reaction zone, should be more sensitive towards the trimer than towards the dimer, the absence of sulfuric acid trimer signals argues against a significant bias in the data due to charged ambient clusters.

3.8 Highly oxidized organic molecules (HOM)

Recently, the rapid autooxidation of atmospherically relevant organic molecules, such as isoprene and monoterpenes, was described (Crounse et al., 2013; Ehn et al., 2014). There is evidence that these HOM are involved in the formation of secondary aerosol and can even promote the formation of new aerosol particles (Jokinen et al., 2015; Kirkby et al., 2016). Nitrate chemical ionization mass spectrometry is capable of detecting a suite of HOM when the O:C-ratio is high (e.g. > ~0.6 for C10 and > ~0.35 for C19/C20 compounds) through association of an NO_3^- primary ion (Ehn et al., 2014), while other ionization techniques are more selective towards less oxidized compounds (Aljawhary et al., 2013). Many recent publications report peak lists for different compounds identified from chamber or ambient measurements with nitrate chemical ionization (Ehn et al., 2012; Kulmala et al., 2013; Ehn et al., 2014; Mutzel et al., 2015; Praplan et al., 2015; Jokinen et al., 2015; Kirkby et al., 2016). The species from the previous studies are mainly C10 (containing 10 carbon atoms) or C20 (containing 19 or 20 carbon atoms) compounds originating from reactions between monoterpenes (in most cases from α-pinene) and ozone and/or OH.

The C10 compounds can be further segregated in HOM radicals (RO_2, i.e. $C_{10}H_{15}O_{i\geq6}$), HOM monomers ($C_{10}H_{14}O_{i\geq7}$ and $C_{10}H_{16}O_{i\geq6}$) and HOM involving reactions with nitrate ($C_{10}H_{15}NO_{i\geq7}$ and $C_{10}H_{16}N_2O_{i\geq8}$) (Jokinen et al., 2014). Dimers (C19/C20 compounds) originate from reactions among HOM RO_2 radicals (Ehn et al., 2014).

The spectra were evaluated according to the peak list shown in Table 2 regarding HOM. It should be noted that the listed compounds represent some fraction of the observed signal in the monomer and dimer region although not all of the peaks that are present are identified yet. Figure 7 shows a comparison

Atmos. Chem. Phys. Discuss., doi:10.5194/acp-2016-294, 2016
Manuscript under review for journal Atmos. Chem. Phys.
Published: 6 June 2016

between the average day-time and the average night time spectra for the mass to charge range between *m*/z 300 and 650. According to Fig. 7 the main difference between day and night are the significantly higher signals in the dimer region during the night.

Fig. 8 shows the diurnal variation of the HOM (separated into HOM radicals, HOM monomers, HOM nitrates and HOM dimers according to Table 2) together with other parameters (NO, NO_2, O_3 and global radiation). One striking feature is the pronounced maximum concentration of HOM dimers during the night. During the day when the global radiation shows values above zero the dimer signals drop by about one order of magnitude and reach levels, which are close to the detection limit of the instrument. The low day-time dimer concentrations are probably due to enhanced NO, HO_2 and $R'O_2$ concentrations during the day. These compounds can react with HOM RO_2 radicals and thereby inhibit the formation of dimers; which are a result of the reaction between two RO_2 radicals. As can be seen from Fig. 8 the NO concentration peaks in the morning. HO_2 was not measured but typically peaks around noon or in the later afternoon (Monks, 2005). Direct photolysis of HOM dimers has to our knowledge not been reported in the literature but could in principle also explain the dimer pattern seen in Fig. 8.

The HOM monomer signal (Fig. 8) does not show a pronounced diurnal cycle, only in the early morning the signals are reduced by about 50% compared to the daily average. Slightly higher values around noon could be explained by the higher O_3 and OH concentrations during mid-day, which lead to enhanced formation of HOM through reactions between these compounds and monoterpenes (Jokinen et al., 2015; Kirkby et al., 2016). The HOM nitrates, di-nitrates and radicals show almost the same profile as the HOM monomers. This might be expected for the HOM radicals as these can be regarded as the precursors for the HOM monomers but the fact that the HOM nitrates follow an almost identical pattern is somewhat surprising as the NO mixing ratio shows a different profile and is thought to be involved in the formation of the HOM nitrates. However, further involvement of e.g. OH, HO_2 and $R'O_2$ in the HOM formation should also play a role and therefore influence their diurnal pattern. The elucidation of the HOM formation mechanisms is beyond the scope of this article and will therefore not be discussed further. More field and chamber experiments are needed to identify the influence of different trace gases and radicals on the formation and concentration of HOM.

3.9 Particle formation rates

The presence of small particles (< ~20 nm) was observed on almost every day during the campaign. However, often nanometer-sized particles appeared suddenly without clear growth from the smallest size the nDMA covered (slightly above 3 nm). In total there were seven events where clear growth was detectable and these events were the only ones for which a new particle formation rate (J) was derived.

In accordance with other previous studies (Metzger et al., 2010; Kirkby et al., 2011) we have first derived a new particle formation rate at a larger mobility diameter d_{p2} (2.5 nm in the present study), which was corrected to a smaller diameter of d_{p1} = 1.7 nm in a second step. The formation rate J_{dp2} is

Atmos. Chem. Phys. Discuss., doi:10.5194/acp-2016-294, 2016
Manuscript under review for journal Atmos. Chem. Phys.
Published: 6 June 2016

obtained from the time derivative of the small particle concentration, which follows from the difference in particle concentrations ($N_{2.5\text{-}10}$) measured by the TSI 3776 (cut-off diameter of 2.5 nm) and a TSI 3010 (cut-off diameter of 10 nm):

$$J_{d_{p2}} = \frac{dN_{2.5-10}}{dt} + CS_{d_{p2}} \cdot N_{2.5-10}. \quad (7)$$

The second term on the right-hand side in equation (7) accounts for the loss of small particles on particles larger than 2.5 nm. The coagulation sink CS_{dp2} is calculated from the particle size distribution measured by the nDMA and the SMPS. The second step involves an exponential correction to obtain the particle formation rate at the smaller size, J_{dp1}, by taking into account the coagulation sink and the growth rate (GR) of particles (Lehtinen et al., 2007):

$$J_{d_{p1}} = J_{d_{p2}} \cdot exp\left(\frac{CS_{d_{p1}}}{GR} \cdot dp_1 \cdot \gamma\right). \quad (8)$$

The factor γ is defined as follows (Lehtinen et al., 2007):

$$\gamma = \frac{1}{s+1} \cdot \left(\left(\frac{d_{p2}}{d_{p1}}\right)^{s+1} - 1\right), \quad (9)$$

where s is the slope of the coagulation sink as a function of size for the size range between d_{p1} and d_{p2} ($s = \log(CS_{dp2}/CS_{dp1})/\log(d_{p2}/d_{p1})$). The value of s can be derived from the measured particle size distribution and was found to be around -1.6 for the present study, which is in good agreement with the values reported by Lehtinen et al. (2007). The growth rate was derived from the nDMA measurements in the size range between 3 and 10 nm by fitting a Gaussian function to the particle size distribution to determine the mode diameter for all measured size distributions. Applying a linear fit to the mode diameter as a function of time yields the GR used in equation (8) (Hirsikko et al., 2005). Errors are calculated by taking into account the statistical variation of the particle formation rates J_{dp2} as well as systematic errors on GR (factor of 2), d_{p2} (factor 1.3) and CS (factor 1.5).

Figure 9 shows a comparison between J_{dp1} from this study, data from other field studies and formation rates from CLOUD chamber studies for the system of sulfuric acid, dimethylamine and water at 278 K (Almeida et al., 2013) as well as for oxidized organic compounds with sulfuric acid and water (Riccobono et al., 2014).

4. Discussion

Atmos. Chem. Phys. Discuss., doi:10.5194/acp-2016-294, 2016
Manuscript under review for journal Atmos. Chem. Phys.
Published: 6 June 2016

Atmospheric Chemistry and Physics Discussions

By comparing time periods where significant new particle formation (NPF) occurred to time periods where no NPF was observed, some conclusions can be drawn about the relevance of certain parameters regarding NPF. Figure 10 shows a comparison for a variety of parameters by comparing nucleation days to no nucleation days (red bars) and periods with high sulfuric acid dimer concentrations to no nucleation days when there are also no high dimer concentrations (blue bars).

It is evident from Fig. 10 that sulfuric acid is on average a factor of 2 to 2.5 higher on days with nucleation; although the variability is rather high (error bars take into account the standard deviations of a parameter both for the nucleation days and the no nucleation days). The enhanced sulfuric acid concentrations confirm the importance of this compound regarding NPF, which has also been shown in numerous other studies (e.g. Weber et al., 1997; Kulmala et al., 2004; Fiedler et al., 2005; Kuang et al., 2008). The OH concentration and the global radiation are also enhanced during nucleation, which is not surprising given the fact that the parameters H_2SO_4, OH and global radiation are connected. The relative humidity is generally lower during nucleation periods, which has also been reported in previous studies (Hamed et al., 2011; Nieminen et al., 2015).

Regarding amines and ammonia Fig. 10 reveals an anti-correlation between their concentration and the occurrence of NPF or sulfuric acid dimer formation (factor 2 to 5 lower during nucleation). However, this does not necessarily mean that these compounds inhibit the formation of particles. On the contrary, it could mean that amines and ammonia are efficiently taken up by small clusters and therefore are also involved in the formation of new particles. Unlike sulfuric acid, amines and ammonia are not produced in the gas phase and therefore their concentration will decrease with increasing distance from their sources depending on the condensation sink. During nucleation the condensation sink is slightly enhanced (Fig. 10), probably because of the newly formed particles. However, the *CS* is only calculated for particles larger than 3 nm. Also smaller particles and sulfuric acid clusters can contain amines (Kürten et al., 2014) and even the sulfuric acid monomer can be bound to dimethylamine (Ortega et al., 2012; Kürten et al., 2014). Therefore, continuous production of sulfuric acid and its clusters will lead to a depletion of amines away from their sources, although no mixed clusters of sulfuric acid and amines could be observed; this is probably the case because their concentrations were too low to be measured with the CI-APi-TOF. As sulfuric acid concentrations are high during nucleation this could explain the low amine values. Efficient uptake of amines in the particle phase has also been reported in a previous field study (You et al., 2014). In addition, the limited pool of amines can also be the explanation for the relatively low slope from Fig. 6 (sulfuric acid dimer vs. monomer) for some of the periods with elevated sulfuric acid dimer concentrations. If the sulfuric acid concentration increases, the ratio of the free (unbound) amine to sulfuric acid concentration drops, and there are fewer amines available to stabilize the sulfuric acid dimers. This is a different situation compared to the CLOUD experiment where the amine to sulfuric acid concentration was maintained at a ratio of ~100 over the entire duration of the experiments. However, from these observations we cannot unambiguously conclude if the amines are involved in the very first steps of nucleation, or if they are depleted due to clusters, which do not need

Atmos. Chem. Phys. Discuss., doi:10.5194/acp-2016-294, 2016
Manuscript under review for journal Atmos. Chem. Phys.
Published: 6 June 2016

Atmospheric Chemistry and Physics Discussions

the help of amines in order to nucleate. One other aspect that could explain the low amine ratios is the somewhat enhanced OH concentration during the nucleation days, as amines react with OH. However, the life-time of amines regarding their reactions with OH is on the order of hours (Ge et al., 2011), whereas the uptake on particles is significantly faster (if *CS* is on the order of 10^{-3} to 10^{-2} s^{-1}).

Regarding the possibility that sulfuric acid and amines can explain the observed nucleation it has to be noted that no clusters involving more than two sulfuric acid molecules could be observed. In the following we will calculate the maximum expected sulfuric acid trimer concentration and discuss what parameters can lower this concentration. The maximum measured sulfuric acid dimer concentration is around 1×10^5 molecule cm^{-3} for a sulfuric acid monomer concentration of 1×10^7 molecule cm^{-3}. A sulfuric acid trimer will be formed through the collision between a monomer and a dimer (collision rate $K_{1,2}$), whereas the loss rate of the trimer is defined by the sum of the condensation sink (*CS*) and its evaporation rate ($k_{e,3}$). At steady-state this would yield the following equation for the trimer concentration N_3 as function of the monomer and dimer concentrations N_1 and N_2 (for simplicity this neglects a potential contribution from tetramer evaporation):

$$N_3 = \frac{K_{1,2}\cdot N_1\cdot N_2}{CS+k_{e,3}}. \quad (10)$$

Using a value of 5×10^{-10} $molecule^{-1}$ cm^3 s^{-1} for $K_{1,2}$ and a condensation sink (*CS*) of 5×10^{-3} s^{-1} for the above mentioned monomer and dimer concentrations would yield a trimer concentration of 1×10^5 molecule cm^{-3} if the trimer evaporation rate would be zero. This concentration should be detectable with our CI-APi-TOF. The fact that we do not see the trimer could indicate that the trimer evaporation rate is non-zero. For a high amine to sulfuric acid ratio nucleation proceeds at or close to the kinetic limit (Jen et al., 2014; Kürten et al., 2014). However, if the amine concentration is not very high, not every trimer that is formed would be stable (as it is the case for a favored acid-base ratio, see Ortega et al., 2012) and therefore could evaporate rapidly. This would result in lower trimer concentrations, which could be below the detection limit of the CI-APi-TOF. From this perspective the absence of larger sulfuric acid amine clusters is not necessarily an indication that this system is not responsible for new particle formation. In other regions where the sulfuric acid and amine mixing ratios are even higher (i.e. very close to amine sources) such clusters can be observable (Zhao et al., 2011).

The C10 and C20 signals for NPF and no nucleation days are not significantly different (Fig. 10). This can be interpreted in different ways: (1) the HOM are not important in terms of NPF, (2) HOM are generally high enough and it needs just enough sulfuric acid to initiate nucleation involving HOM, or (3) „HOM“ is too broadly defined and only a subgroup of HOM is involved in the nucleation but currently we cannot distinguish this group. Neither of the possibilities can be proven right or wrong. However, what can be said is that it is unlikely that the identified HOM alone are capable of producing new particles to a significant extent at the conditions of the present study. The HOM dimer concentrations (Fig. 8) are significantly higher during the night than during the day. Nevertheless, no

night-time nucleation is observed. This could be interpreted as an indication that if HOM are involved in NPF it requires additional compounds such as sulfuric acid to initiate nucleation. Alternative explanations for the absence of night-time nucleation could be the suppression of the formation of HOM that can nucleate by NO_3 during the night, or low [OH], which is required for the formation of nucleating HOM.

Kulmala et al. (2013) proposed that $C_{10}H_{15}NO_8$ (detected as a cluster with NO_3^- at 339.0681 Th) could be important because NPF correlated even better with this compound compared to sulfuric acid. During nucleation days this compound is only slightly elevated (Fig. 10) and this could be due to the generally higher OH levels although the exact formation mechanism of $C_{10}H_{15}NO_8$ has to our knowledge not been reported yet. During nucleation, no mixed clusters between sulfuric acid and HOM could be identified. However, this also does not rule out their existence as the concentrations could be below the CI-APi-TOF detection limit, or a low charging efficiency with the nitrate primary ion could prevent their detection. Furthermore, not all signals are identified yet.

The observed particle formation rates (Fig. 9) are consistent with the rates observed at other sites, although being at the upper end of the typical ranges that have been previously measured. The present data seem to agree a bit better to CLOUD chamber data for the system of sulfuric acid, water and dimethylamine (Almeida et al., 2013) compared to data for the system of sulfuric acid, water and oxidized organics from pinanediol (Riccobono et al., 2014). However, a direct comparison is difficult as the conditions between this ambient study and the CLOUD chamber experiments are not identical (with respect to *T*, *RH*, *CS*, amine mixing ratios, HOM concentrations, etc.).

5. Summary

In spring 2014 (May 18 to June 7) a field campaign was conducted at a rural site in central Germany (Vielbrunn/Odenwald). The measurement site was in proximity (within 450 to 1100 m distance) of three larger dairy farms. The perspective of this campaign was to evaluate if there is a connection between new particle formation and the concentration of amines and/or ammonia. Furthermore, the impact of highly oxidized organic molecules (HOM) from surrounding forests was investigated. A nitrate Chemical Ionization-Atmospheric Pressure interface-Time Of Flight mass spectrometer (CI-APi-TOF) was used to identify gas-phase compounds and clusters. Particle counters and differential mobility analyzers were used to characterize the aerosol size distribution and number density. The following conclusions can be drawn from our measurements:

- Nitrate CI-APi-TOF can be used to measure sulfuric acid, iodic acid, amines, a nitrosamine, ammonia and HOM; the measurement of iodic acid, ammonia and the nitrosamine has not been described before; the method is therefore even more versatile than previously thought and well suited to study all of the above-mentioned compounds during field measurements.

- The sulfuric acid concentration can be well described by proxies (SO_2, global radiation, RH and *CS* or just by SO_2 and global radiation) for this site with a similar accuracy as reported in a previous study (Mikkonen et al., 2011).
- Significant sulfuric acid dimer concentrations were measured; it is, however, not clear what compound stabilizes the neutral dimers; larger sulfuric acid clusters (trimer and beyond) were not observed.
- Amines (C1-, C2-, C3-, C4- and C6-amines) are present at estimated mixing ratios between approximately 1 and 5 pptv, which is consistent with other studies; the C4- and C6-amines as well as ammonia show a diurnal variation, which follows the temperature profile.
- Iodine has been observed (probably iodic acid) on every day, somewhat surprising for a continental site located more than 400 km away from the ocean; the nitrate CI-APi-TOF has a high sensitivity towards iodic acid and its presence indicates long-range transport of iodine containing substances (although a local source cannot entirely be ruled out); using OH concentrations also OIO concentrations can be estimated; however, both [HIO_3] (~3×10^5 molecule cm^{-3}) and [OIO] (~5×10^6 molecule cm^{-3}) are probably too low to affect new particle formation significantly at this site.
- The diurnal pattern of HOM dimers shows maximum concentrations during the night but no night-time nucleation is observed; the day-time concentration could be low due to the presence of NO and/or HO_2 which suppress the HOM dimer formation.
- Relatively high particle formation rates are found, which are rather at the upper end of the atmospheric observations for other rural sites; the rates are compatible with CLOUD chamber data both for the systems of sulfuric acid, water and dimethylamine (Almeida et al., 2013), as well as for a system involving sulfuric acid, water and oxidized organics (Riccobono et al., 2014); no definitive answer can be given which system is more relevant.
- Nucleation seems to be favored on days with relatively low RH and high sulfuric acid; an anti-correlation with the amine and ammonia signals is observed, this could be due to efficient uptake of these compounds on clusters and particles during NPF as amines and ammonia are not produced in the gas-phase.

The above bullet points seem to support recent findings about the relevance of amines in terms of NPF and early growth (Chen et al., 2012; Almeida et al., 2013; Kulmala et al., 2013; Lehtipalo et al., 2016). However, it cannot be unambiguously concluded that amines are more relevant for NPF than HOM at this site because no nucleating clusters could be directly observed. More studies like the present one are necessary in the future to obtain better statistics about the parameters relevant for NPF (Fig. 10). Ideally, such measurements should include further instrumentation including a PSM (Vanhanen et al., 2011) for the measurement of clusters and small particles (< 3 nm), an APi-TOF (Junninen et al., 2010) for better identification of charged nucleating clusters, an instrument for HO_x/RO_x measurements (Mauldin et al., 2016) and an instrument for sensitive amine measurements capable of speciating the amines.

Atmos. Chem. Phys. Discuss., doi:10.5194/acp-2016-294, 2016
Manuscript under review for journal Atmos. Chem. Phys.
Published: 6 June 2016

Atmospheric Chemistry and Physics Discussions

Acknowledgments

We thank the German Weather Service (Deutscher Wetterdienst, DWD) for providing infrastructure and meteorological data. Funding from the German Federal Ministry of Education and Research (grant no. 01LK1222A) and the Marie Curie Initial Training Network "CLOUD-TRAIN" (grant no. 316662) is gratefully acknowledged.

778 **References**

779

780 Aljawhary, D., Lee, A. K. Y., and Abbatt, J. P. D.: High-resolution chemical ionization mass
781 spectrometry (ToF-CIMS): application to study SOA composition and processing, Atmos. Meas. Tech.,
782 6, 3211–3224, doi: 10.5194/amt-6-3211-2013, 2013.

783

784 Almeida, J., Schobesberger, S., Kürten, A., Ortega, I. K., Kupiainen-Määttä, O., Praplan, A. P., Adamov,
785 A., Amorim, A., Bianchi, F., Breitenlechner, M., David, A., Dommen, J., Donahue, N. M., Downard,
786 A., Dunne, E. M., Duplissy, J., Ehrhart, S., Flagan, R. C., Franchin, A., Guida, R., Hakala, J., Hansel,
787 A., Heinritzi, M., Henschel, H., Jokinen, T., Junninen, H., Kajos, M., Kangasluoma, J., Keskinen, H.,
788 Kupc, A., Kurtén, T., Kvashin, A. N., Laaksonen, A., Lehtipalo, K., Leiminger, M., Leppä, J., Loukonen,
789 V., Makhmutov, V., Mathot, S., McGrath, M. J., Nieminen, T., Olenius, T., Onnela, A., Petäjä, T.,
790 Riccobono, F., Riipinen, I., Rissanen, M., Rondo, L., Ruuskanen, T., Santos, F. D., Sarnela, N.,
791 Schallhart, S., Schnitzhofer, R., Seinfeld, J. H., Simon, M., Sipilä, M., Stozhkov, Y., Stratmann, F.,
792 Tomé, A., Tröstl, J., Tsagkogeorgas, G., Vaattovaara, P., Viisanen, Y., Virtanen, A., Vrtala, A., Wagner,
793 P. E., Weingartner, E., Wex, H., Williamson, C., Wimmer, D., Ye, P., Yli-Juuti, T., Carslaw, K. S.,
794 Kulmala, M., Curtius, J., Baltensperger, U., Worsnop, D. R., Vehkamäki, H., and Kirkby, J.: Molecular
795 understanding of sulphuric acid-amine particle nucleation in the atmosphere, Nature, 502, 359–363, doi:
796 10.1038/nature12663, 2013.

797

798 Berndt, T., Jokinen, T., Sipilä, M., Mauldin III, R. L. Herrmann, H., Stratmann, F., Junninen, H., and
799 Kulmala, M: H_2SO_4 formation from the gas-phase reaction of stabilized Criegee Intermediates with SO_2:
800 Influence of water vapour content and temperature, Atmos. Env., 89, 603–612, doi:
801 10.1016/j.atmosenv.2014.02.062, 2014.

802

803 Berresheim, H., Elste, T., Plass-Dülmer, C., Eisele, F. L., and Tanner, D. J.: Chemical ionization mass
804 spectrometer for long-term measurements of atmospheric OH and H_2SO_4, Int. J. Mass Spectrom., 202,
805 91–109, doi: 10.1016/S1387-3806(00)00233-5, 2000.

806

807 Blake, R. S., Monks, P. S., and Ellis, A. M.: Proton-Transfer Reaction Mass Spectrometry, Chem. Rev.,
808 109, 861–896, doi: 10.1021/cr800364q, 2009.

809

810 Boy, M., Mogensen, D., Smolander, S., Zhou, L., Nieminen, T., Paasonen, P., Plass-Dülmer, C., Sipilä,
811 M., Petäjä, T., Mauldin, L., Berresheim, H., and Kulmala, M.: Oxidation of SO_2 by stabilized Criegee
812 intermediate (sCI) radicals as a crucial source for atmospheric sulfuric acid concentrations, Atmos.
813 Chem. Phys., 13, 3865–3879, doi: 10.5194/acp-13-3865-2013, 2013.

814

Cappellin, L., Karl, T., Probst, M., Ismailova, O., Winkler, P. M., Soukoulis, C., Aprea, E., Märk, T. D., Gasperi, F., and Biasioli, F.: On quantitative determination of volatile organic compound concentrations using proton transfer reaction time-of-flight mass spectrometry, Env. Sci. Technol., 46, 2283–2290, doi: 10.1021/es203985t, 2012.

Chang, D., Song, Y., and Liu, B.: Visibility trends in six megacities in China 1973–2007, Atmos. Res., 94, 161–167, doi: 10.1016/j.atmosres.2009.05.006, 2009.

Chen, M., Titcombe, M., Jiang, J., Jen, C., Kuang, C., Fischer, M. L., Eisele, F. L., Siepmann, J. I., Hanson, D. R., Zhao, J., and McMurry, P. H.: Acid–base chemical reaction model for nucleation rates in the polluted atmospheric boundary layer, P. Natl. Acad. Sci. USA, 109, 18713–18718, doi: 10.1073/pnas.1210285109, 2012.

Crounse, J. D., Nielsen, L. B., Jørgensen, S., Kjaergaard, H. G., and Wennberg, P. O.: Autooxidation of organic compounds in the atmosphere, J. Phys. Chem. Lett., 4, 3513−3520, doi: 10.1021/jz4019207, 2013.

Ehn, M., Kleist, E., Junninen, H., Petäjä, T., Lönn, G., Schobesberger, S., Dal Maso, M., Trimborn, A., Kulmala, M., Worsnop, D. R., Wahner, A., Wildt, J., and Mentel, Th. F.: Gas phase formation of extremely oxidized pinene reaction products in chamber and ambient air, Atmos. Chem. Phys., 12, 5113–5127, doi: 10.5194/acp-12-5113-2012, 2012.

Ehn, M., Thornton, J. A., Kleist, E., Sipilä, M., Junninen, H., Pullinen, I., Springer, M., Rubach, F., Tillmann, R., Lee, B., Lopez-Hilfiker, F., Andres, S., Acir, I.-H., Rissanen, M., Jokinen, T., Schobesberger, S., Kangasluoma, J., Kontkanen, J., Nieminen, T., Kurtén, T., Nielsen, L. B., Jørgensen, S., Kjaergaard, H. G., Canagaratna, M., Dal Maso, M., Berndt, T., Petäjä, T., Wahner, A., Kerminen, V.-M., Kulmala, M., Worsnop, D. R., Wildt, J., and Mentel, T. F.: A large source of low-volatility secondary organic aerosol, Nature, 506, 476–479, doi: 10.1038/nature13032, 2014.

Eisele, F. L., and Tanner, D. J.: Measurement of the gas phase concentration of H_2SO_4 and methane sulfonic acid and estimates of H_2SO_4 production and loss in the atmosphere, J. Geophys. Res., 98, D5, 9001–9010, doi: 10.1029/93JD00031, 1993.

Eisele, F. L., Lovejoy, E. R., Kosciuch, E., Moore, K. F., Mauldin III, R. L., Smith, J. N., McMurry, P. H., and Iida, K.: Negative atmospheric ions and their potential role in ion-induced Nucleation, J. Geophys. Res., 111, D04305, doi: 10.1029/2005JD006568, 2006.

852 Fiedler, V., Dal Maso, M., Boy, M., Aufmhoff, H., Hoffmann, J., Schuck, T., Birmili, W., Hanke, M.,
853 Uecker, J., Arnold, F., and Kulmala, M.: The contribution of sulphuric acid to atmospheric particle
854 formation and growth: a comparison between boundary layers in Northern and Central Europe, Atmos.
855 Chem. Phys., 5, 1773–1785, doi: 10.5194/acp-5-1773-2005, 2005.
856
857 Freshour, N. A., Carlson, K. K., Melka, Y. A., Hinz, S., Panta, B., and Hanson, D. R.: Amine permeation
858 sources characterized with acid neutralization and sensitivities of an amine mass spectrometer, Atmos.
859 Meas. Tech., 7, 3611–3621, doi: 10.5194/amt-7-3611-2014, 2014.
860
861 Ge, X., Wexler, A. S., and Clegg, S. L.: Atmospheric amines – Part I. A review, Atmos. Env., 45, 524–
862 546, doi: 10.1016/j.atmosenv.2010.10.012, 2011.
863
864 Geron, C., Rasmussen, R., Arnts, R. R., and Guenther, A.: A review and synthesis of monoterpene
865 speciation from forests in the United States, Atmos. Env., 34, 1761–1781, doi: 10.1016/S1352-
866 2310(99)00364-7, 2000.
867
868 Glasoe, W. A., Volz, K., Panta, B., Freshour, N., Bachman, R., Hanson, D. R., McMurry, P. H., and Jen,
869 C.: Sulfuric acid nucleation: An experimental study of the effect of seven bases, J. Geophys. Res.
870 Atmos., 120, 1933–1950, doi: 10.1002/2014JD022730, 2015.
871
872 Glasson, W. A.: An experimental evaluation of atmospheric nitrosamine formation, Environ. Sci.
873 Technol., 13, 1145–1146, doi: 10.1021/es60157a017, 1979.
874
875 Grosjean, D.: Atmospheric chemistry of toxic contaminants. 6. Nitrosamines: Dialkyl nitrosamines and
876 nitrosomorpholine, J. Air Waste Manag. Assoc., 41, 306–311, doi: 10.1080/10473289.1991.10466847,
877 1991.
878
879 Hamed, A., Korhonen, H., Sihto, S.-L., Joutsensaari, J., Järvinen, H., Petäjä, T., Arnold, F., Nieminen,
880 T., Kulmala, M., Smith, J. N., Lehtinen, K. E. J., and Laaksonen, A.: The role of relative humidity in
881 continental new particle formation, J. Geophys. Res., 116, D03202, doi: 10.1029/2010JD014186, 2011.
882
883 Hanson, D. R., and Eisele, F. L.: Measurement of prenucleation molecular clusters in the NH_3, H_2SO_4,
884 H_2O system, J. Geophys. Res., 107, D12, 4158, doi: 10.1029/2001JD001100, 2002.
885
886 Hanson, D. R., and Lovejoy, E. R.: Measurement of the thermodynamics of the hydrated dimer and
887 trimer of sulfuric acid, J. Phys. Chem. A, 110, 9525–9528, doi: 10.1021/jp062844w, 2006.
888

889 Hanson, D. R., McMurry, P. H., Jiang, J., Tanner, D., and Huey, L. G.: Ambient pressure proton transfer
890 mass spectrometry: detection of amines and ammonia, Environ. Sci. Technol., 45, 8881–8888, doi:
891 10.1021/es201819a, 2011.
892
893 Hellén, H., Kieloaho, A.-J., and Hakola, H.: Gas-phase alkyl amines in urban air; comparison with a
894 boreal forest site and importance for local atmospheric chemistry, Atmos. Env., 94, 192–197, doi:
895 10.1016/j.atmosenv.2014.05.029, 2014.
896
897 Hirsikko, A., Laakso, L., Hõrrak, U., Aalto, P. P., Kerminen, V.-M., and Kulmala, M.: Annual and size
898 dependent variation of growth rates and ion concentrations in boreal forest, Boreal Env. Res., 10, 357–
899 369, 2005.
900
901 Heinritzi, M., Simon, M., Steiner, G., Wagner, A. C., Kürten, A., Hansel, A., and Curtius, J.:
902 Characterization of the mass-dependent transmission efficiency of a CIMS, Atmos. Meas. Tech., 9,
903 1449–1460, doi: 10.5194/amt-9-1449-2016, 2016.
904
905 Janson, R., and de Serves, C.: Acetone and monoterpene emissions from the boreal forest in northern
906 Europe, Atmos. Env., 35, 4629–4637, doi: 10.1016/S1352-2310(01)00160-1, 2001.
907
908 Jen, C., McMurry, P. H., and Hanson, D. R.: Stabilization of sulfuric acid dimers by ammonia,
909 methylamine, dimethylamine, and trimethylamine, J. Geophys. Res. Atmos., 119, 7502–7514, doi:
910 10.1002/2014JD021592, 2014.
911
912 Jen, C. N., Bachman, R., Zhao, J., McMurry, P. H., and Hanson, D. R.: Diamine-sulfuric acid reactions
913 are a potent source of new particle formation, Geophys. Res. Lett., 43, 867–873, doi:
914 10.1002/2015GL066958, 2016.
915
916 Jiang, J., Zhao, J., Chen, M., Eisele, F. L., Scheckman, J., Williams, B. J., Kuang, C., and McMurry, P.
917 H.: First measurements of neutral atmospheric cluster and 1-2 nm particle number size distributions
918 during nucleation events, Aerosol Sci. Technol., 45, ii–v, doi: 10.1080/02786826.2010.546817, 2011.
919
920 Jokinen, T., Sipilä, M., Junninen, H., Ehn, M., Lönn, G., Hakala, J., Petäjä, T., Mauldin III, R. L.,
921 Kulmala, M., and Worsnop, D. R.: Atmospheric sulphuric acid and neutral cluster measurements using
922 CI-APi-TOF, Atmos. Chem. Phys., 12, 4117–4125, doi: 10.5194/acp-12-4117-2012, 2012.
923
924 Jokinen, T., Sipilä, M., Richters, S., Kerminen, V.-M., Paasonen, P., Stratmann, F., Worsnop, D.,
925 Kulmala, M., Ehn, M., Herrmann, H., and Berndt, T.: Rapid autooxidation forms highly oxidized RO_2

radicals in the atmosphere, Angew. Chem. Int. Ed., 53, 14596 –14600, doi: 10.1002/anie.201408566, 2014.

Jokinen, T., Berndt, T., Makkonen, R., Kerminen, V.-M., Junninen, H., Paasonen, P., Stratmann, F., Herrmann, H., Guenther, A. B., Worsnop, D. R., Kulmala, M., Ehn, M., and Sipilä, M.: Production of extremely low volatile organic compounds from biogenic emissions: Measured yields and atmospheric implications, P. Natl. Acad. Sci. USA, doi: 10.1073/pnas.1423977112, 2015.

Junninen, H., Ehn, M., Petäjä, T., Luosujärvi, L., Kotiaho, T., Kostiainen, R., Rohner, U., Gonin, M., Fuhrer, K., Kulmala, M., and Worsnop, D. R.: A high-resolution mass spectrometer to measure atmospheric ion composition, Atmos. Meas. Tech., 3, 1039–1053, doi: 10.5194/amt-3-1039-2010, 2010.

Kirkby, J., Curtius, J., Almeida, J., Dunne, E., Duplissy, J., Ehrhart, S., Franchin, A., Gagné, S., Ickes, L., Kürten, A., Kupc, A., Metzger, A., Riccobono, F., Rondo, L., Schobesberger, S., Tsagkogeorgas, G., Wimmer, D., Amorim, A., Bianchi, F., Breitenlechner, M., David, A., Dommen, J., Downard, A., Ehn, M., Flagan, R.C., Haider, S., Hansel, A., Hauser, D., Jud, W., Junninen, H., Kreissl, F., Kvashin, A., Laaksonen, A., Lehtipalo, K., Lima, J., Lovejoy, E. R., Makhmutov, V., Mathot, S., Mikkilä, J., Minginette, P., Mogo, S., Nieminen, T., Onnela, A., Pereira, P., Petäjä, T., Schnitzhofer, R., Seinfeld, J. H., Sipilä, M., Stozhkov, Y., Stratmann, F., Tomé, A., Vanhanen, J., Viisanen, Y., Vrtala, A., Wagner, P. E., Walther, H., Weingartner, E., Wex, H., Winkler, P. M., Carslaw, K. S., Worsnop, D. R., Baltensperger, U., and Kulmala, M.: Role of sulphuric acid, ammonia and galactic cosmic rays in atmospheric aerosol nucleation, Nature, 476, 429–435, doi: 10.1038/nature10343, 2011.

Kirkby, J., Duplissy, J., Sengupta, K., Frege, C., Gordon, H., Williamson, C., Heinritzi, M., Simon, M., Yan, C., Almeida, J., Tröstl, J., Nieminen, T., Ortega, I. K., Wagner, R., Adamov, A., Amorim, A., Bernhammer, A.-K., Bianchi, F., Breitenlechner, M., Brilke, S., Chen, X., Craven, J., Dias, A., Ehrhart, S., Flagan, R. C., Franchin, A., Fuchs, C., Guida, R., Hakala, J., Hoyle, C. R., Jokinen, T., Junninen, H., Kangasluoma, J., Kim, J., Krapf, M., Kürten, A., Laaksonen, A., Lehtipalo, K., Makhmutov, V., Mathot, S., Molteni, U., Onnela, A., Peräkylä, O., Piel, F., Petäjä, T., Praplan, A. P., Pringle, K., Rap, A., Richards, N. A. D., Riipinen, I., Rissanen, M. P., Rondo, L., Sarnela, N., Schobesberger, S., Scott, C. E., Seinfeld, J. H., Sipilä, M., Steiner, G., Stozhkov, Y., Stratmann, F., Tomé, A., Virtanen, A., Vogel, A. L., Wagner, A., Wagner, P. E., Weingartner, E., Wimmer, D., Winkler, P. M., Ye, P., Zhang, X., Hansel, A., Dommen, J., Donahue, N. M., Worsnop, D. R., Baltensperger, U., Kulmala, M., Carslaw, K. S., and Curtius, J.: Ion-induced nucleation of pure biogenic particles, Nature, 533, 521–526, doi: 10.1038/nature17953, 2016.

962 Kuang, C., McMurry, P. H., McCormick, A. V., and Eisele, F. L.: Dependence of nucleation rates on
963 sulfuric acid vapor concentration in diverse atmospheric locations, J. Geophys. Res., 113, D10209, doi:
964 10.1029/2007JD009253, 2008.
965
966 Kulmala, M., Vehkamäki, H., Petäjä, T., Dal Maso, M., Lauri, A., Kerminen, V.-M., Birmili, W., and
967 McMurry, P. H.: Formation and growth rates of ultrafine atmospheric particles: a review of observations,
968 J. Aerosol Sci., 35, 143–176, doi: 10.1016/j.jaerosci.2003.10.003, 2004.
969
970 Kulmala, M., Kontkanen, J., Junninen, H., Lehtipalo, K., Manninen, H. E., Nieminen, T., Petäjä, T.,
971 Sipilä, M., Schobesberger, S., Rantala, P., Franchin, A., Jokinen, T., Järvinen, E., Äijälä, M.,
972 Kangasluoma, J., Hakala, J., Aalto, P. P., Paasonen, P., Mikkilä, J., Vanhanen, J., Aalto, J., Hakola, H.,
973 Makkonen, U., Ruuskanen, T., Mauldin III, R. L., Duplissy, J., Vehkamäki, H., Bäck, J., Kortelainen,
974 A., Riipinen, I., Kurtén, T., Johnston, M. V., Smith, J. N., Ehn, M., Mentel, T. F., Lehtinen, K. E. J.,
975 Laaksonen, A., Kerminen, V.-M., and Worsnop, D. R.: Direct observations of atmospheric aerosol
976 nucleation, Science, 339, 943–946, doi: 10.1126/science.1227385, 2013.
977
978 Kürten, A., Rondo, L., Ehrhart, S., and Curtius, J.: Performance of a corona ion source for measurement
979 of sulfuric acid by chemical ionization mass spectrometry, Atmos. Meas. Technol., 4, 437−443, doi:
980 10.5194/amt-4-437-2011, 2011.
981
982 Kürten, A., Rondo, L., Ehrhart, S., and Curtius, J.: Calibration of a chemical ionization mass
983 spectrometer for the measurement of gaseous sulfuric acid, J. Phys. Chem. A, 116, 6375−6386, doi:
984 10.1021/jp212123n, 2012.
985
986 Kürten, A., Jokinen, T., Simon, M., Sipilä, M., Sarnela, N., Junninen, H., Adamov, A., Almeida, J.,
987 Amorim, A., Bianchi, F., Breitenlechner, M., Dommen, J., Donahue, N. M., Duplissy, J., Ehrhart, S.,
988 Flagan, R. C., Franchin, A., Hakala, J., Hansel, A., Heinritzi, M., Hutterli, M., Kangasluoma, J., Kirkby,
989 J., Laaksonen, A., Lehtipalo, K., Leiminger, M., Makhmutov, V., Mathot, S., Onnela, A., Petäjä, T.,
990 Praplan, A. P., Riccobono, F., Rissanen, M. P., Rondo, L., Schobesberger, S., Seinfeld, J. H., Steiner,
991 G., Tomé, A., Tröstl, J., Winkler, P. M., Williamson, C., Wimmer, D., Ye, P., Baltensperger, U.,
992 Carslaw, K. S., Kulmala, M., Worsnop, D. R., and Curtius, J.: Neutral molecular cluster formation of
993 sulfuric acid-dimethylamine observed in real-time under atmospheric conditions, P. Natl. Acad. Sci.
994 USA, 111, 15019–15024, doi: 10.1073/pnas.1404853111, 2014.
995
996 Kürten, A., Münch, S., Rondo, L., Bianchi, F., Duplissy, J., Jokinen, T., Junninen, H., Sarnela, N.,
997 Schobesberger, S., Simon, M., Sipilä, M., Almeida, J., Amorim, A., Dommen, J., Donahue, N. M.,
998 Dunne, E. M., Flagan, R. C., Franchin, A., Kirkby, J., Kupc, A., Makhmutov, V., Petäjä, T., Praplan, A.

P., Riccobono, F., Steiner, G., Tomé, A., Tsagkogeorgas, G., Wagner, P. E., Wimmer, D., Baltensperger, U., Kulmala, M., Worsnop, D. R., and Curtius, J.: Thermodynamics of the formation of sulfuric acid dimers in the binary (H_2SO_4–H_2O) and ternary (H_2SO_4–H_2O–NH_3) system, Atmos. Chem. Phys., 15, 10701–10721, doi: 10.5194/acp-15-10701-2015, 2015.

Kürten, A., Bianchi, F., Almeida, J., Kupiainen-Määttä, O., Dunne, E. M., Duplissy, J., Williamson, C., Barmet, P., Breitenlechner, M., Dommen, J., Donahue, N. M., Flagan, R. C., Franchin, A., Gordon, H., Hakala, J., Hansel, A., Heinritzi, M., Ickes, L., Jokinen, T., Kangasluoma, J., Kim, J., Kirkby, J., Kupc, A., Lehtipalo, K., Leiminger, M., Makhmutov, V., Onnela, A., Ortega, I. K., Petäjä, T., Praplan, A. P., Riccobono, F., Rissanen, M. P., Rondo, L., Schnitzhofer, R., Schobesberger, S., Smith, J. N., Steiner, G., Stozhkov, Y., Tomé, A., Tröstl, J., Tsagkogeorgas, G., Wagner, P. E., Wimmer, D., Ye, P., Baltensperger, U., Carslaw, K., Kulmala, M., and Curtius, J.: Experimental particle formation rates spanning tropospheric sulfuric acid and ammonia abundances, ion production rates and temperatures, J. Geophys. Res. Atmos., accepted, doi: 10.1002/2015JD023908, 2016.

Kurtén, T., Loukonen, V., Vehkamäki, H., and Kulmala, M.: Amines are likely to enhance neutral and ion-induced sulfuric acid-water nucleation in the atmosphere more effectively than ammonia, Atmos. Chem. Phys., 8, 4095–4103, doi: 10.5194/acp-8-4095-2008, 2008.

Lehtinen, K. E. J., Dal Maso, M., Kulmala, M., and Kerminen, V.-M.: Estimating nucleation rates from apparent particle formation rates and vice versa: Revised formulation of the Kerminen–Kulmala equation, J. Aerosol Sci., 38, 988–994, doi: 10.1016/j.jaerosci.2007.06.009, 2007.

Lehtipalo, K., Rondo, L., Kontkanen, J., Schobesberger, S., Jokinen, T., Sarnela, N., Kürten, A., Ehrhart, S., Franchin, A., Nieminen, T., Riccobono, F., Sipilä, M., Yli-Juuti, T., Duplissy, J., Adamov, A., Ahlm, L., Almeida, J., Amorim, A., Bianchi, F., Breitenlechner, M., Dommen, J., Downard, A. J., Dunne, E. M., Flagan, R. C., Guida, R., Hakala, J., Hansel, A., Jud, W., Kangasluoma, J., Kerminen, V.-M., Keskinen, H., Kim, J., Kirkby, J., Kupc, A., Kupiainen-Määttä, O., Laaksonen, A., Lawler, M. J., Leiminger, M., Mathot, S., Olenius, T., Ortega, I. K., Onnela, A., Petäjä, T., Praplan, A., Rissanen, M. P., Ruuskanen, T., Santos, F. D., Schallhart, S., Schnitzhofer, R., Simon, M., Smith, J. N., Tröstl, J., Tsagkogeorgas, G., Tomé, A., Vaattovaara, P., Vehkamäki, H., Vrtala, A. E., Wagner, P. E., Williamson, C., Wimmer, D., Winkler, P. M., Virtanen, A., Donahue, N. M., Carslaw, K. S., Baltensperger, U., Riipinen, I., Curtius, J., Worsnop D. R., and Kulmala, M.: The effect of acid-base clustering and ions on the growth of atmospheric nano-particles, Nat. Commun., 7, 11594, doi: 10.1038/ncomms11594, 2016.

1035 Luts, A., Parts, T.-E., Hõrrak, U., Junninen, H., and Kulmala, M.: Composition of negative air ions as a
1036 function of ion age and selected trace gases: Mass- and mobility distribution, J. Aerosol Sci., 42 820–
1037 838, doi: 10.1016/j.jaerosci.2011.07.007, 2011.
1038
1039 Mauldin III, R. L., Berndt, T., Sipilä, M., Paasonen, P., Petäjä, T., Kim, S., Kurtén, T., Stratmann, F.,
1040 Kerminen, V.-M., and Kulmala, M.: A new atmospherically relevant oxidant of sulphur dioxide, Nature,
1041 488, 193-196, doi: 10.1038/nature11278, 2012.
1042
1043 Mauldin III, R. L., Rissanen, M. P., Petäjä, T., and Kulmala, M.: Furthering information from OH and
1044 HO_2 + RO_2 observations using a high resolution time of flight mass spectrometer, Atmos. Meas. Tech.
1045 Discuss., doi: 10.5194/amt-2015-398, 2016.
1046
1047 Merikanto, J., Spracklen, D. V., Mann, G. W., Pickering, S. J., and Carslaw, K. S.: Impact of nucleation
1048 on global CCN, Atmos. Chem. Phys., 9, 8601–8616, doi: 10.5194/acp-9-8601-2009, 2009.
1049
1050 Metzger, A., Verheggen, B., Dommen, J., Duplissy, J., Prevot, A. S. H., Weingartner, E., Riipinen, I.,
1051 Kulmala, M., Spracklen, D. V., Carslaw, K. S., and Baltensperger, U.: Evidence for the role of organics
1052 in aerosol particle formation under atmospheric conditions, P. Natl. Acad. Sci. USA, 107, 6646–6651,
1053 doi: 10.1073/pnas.0911330107, 2010.
1054
1055 Mikkonen, S., Romakkaniemi, S., Smith, J. N., Korhonen, H., Petäjä, T., Plass-Duelmer, C., Boy, M.,
1056 McMurry, P. H., Lehtinen, K. E. J., Joutsensaari, J., Hamed, A., Mauldin III, R. L., Birmili, W., Spindler,
1057 G., Arnold, F., Kulmala, M., and Laaksonen, A.: A statistical proxy for sulphuric acid concentration,
1058 Atmos. Chem. Phys., 11, 11319–11334, doi: 10.5194/acp-11-11319-2011, 2011.
1059
1060 Monks, P. S.: Gas-phase radical chemistry in the troposphere, Chem. Soc. Rev., 34, 376–395, doi:
1061 10.1039/B307982C, 2005.
1062
1063 Mutzel, A., Poulain, L., Berndt, T., Iinuma, Y., Rodigast, M., Böge, O., Richters, S., Spindler, G., Sipilä,
1064 M., Jokinen, T., Kulmala, M., and Herrmann, H.: Highly oxidized multifunctional organic compounds
1065 observed in tropospheric particles: A field and laboratory study, Environ. Sci. Technol., 49, 7754−7761,
1066 doi: 10.1021/acs.est.5b00885, 2015.
1067
1068 Nel, A.: Air pollution–related illness: Effects of particles, Science, 308, 804–806, doi:
1069 10.1126/science.1108752, 2005.
1070

1071 Nieminen, T., Yli-Juuti, T., Manninen, H. E., Petäjä, T., Kerminen, V.-M., and Kulmala, M.: Technical
1072 note: New particle formation event forecasts during PEGASOS–Zeppelin Northern mission 2013 in
1073 Hyytiälä, Finland, Atmos. Chem. Phys., 15, 12385–12396, doi: 10.5194/acp-15-12385-2015, 2015.
1074
1075 Ortega, I. K., Kupiainen, O., Kurtén, T., Olenius, T., Wilkman, O., McGrath, M. J., Loukonen, V., and
1076 Vehkamäki, H.: From quantum chemical formation free energies to evaporation rates, Atmos. Chem.
1077 Phys., 12, 225–235, doi: 10.5194/acp-12-225-2012, 2012.
1078
1079 Ortega, I. K., Olenius, T., Kupiainen-Määttä, O., Loukonen, V., Kurtén, T., and Vehkamäki, H.:
1080 Electrical charging changes the composition of sulfuric acid–ammonia/dimethylamine clusters, Atmos.
1081 Chem. Phys., 14, 7995–8007, doi: 10.5194/acp-14-7995-2014, 2014.
1082
1083 Paasonen, P., Nieminen, T., Asmi, E., Manninen, H. E., Petäjä, T., Plass-Dülmer, C., Flentje, H., Birmili,
1084 W., Wiedensohler, A., Hõrrak, U., Metzger, A., Hamed, A., Laaksonen, A., Facchini, M. C., Kerminen,
1085 V.-M., and Kulmala, M.: On the roles of sulphuric acid and low-volatility organic vapours in the initial
1086 steps of atmospheric new particle formation, Atmos. Chem. Phys., 10, 11223–11242, doi: 10.5194/acp-
1087 10-11223-2010, 2010.
1088
1089 Petäjä, T., Mauldin, III, R. L., Kosciuch, E., McGrath, J., Nieminen, T., Paasonen, P., Boy, M., Adamov,
1090 A., Kotiaho, T., and Kulmala, M.: Sulfuric acid and OH concentrations in a boreal forest site, Atmos.
1091 Chem. Phys., 9, 7435–7448, doi: 10.5194/acp-9-7435-2009, 2009.
1092
1093 Pitts, Jr., J. N., Grosjean, D., Van Cauwenberghe, K., Schmid, J. P., and Fitz, D. R.: Photooxidation of
1094 aliphatic amines under simulated atmospheric conditions: Formation of nitrosamines, nitramines,
1095 amides, and photochemical oxidant, Environ. Sci. Technol., 12, 946–953, doi: 10.1021/es60144a009,
1096 1978.
1097
1098 Plane, J. M. C., Joseph, D. M., Allan, B. J., Ashworth, S. H., and Francisco, J. S.: An experimental and
1099 theoretical study of the reactions OIO + NO and OIO + OH, J. Phys. Chem. A, 110, 93–100, doi:
1100 10.1021/jp055364y, 2006.
1101
1102 Praplan, A. P., Schobesberger, S., Bianchi, F., Rissanen, M. P., Ehn, M., Jokinen, T., Junninen, H.,
1103 Adamov, A., Amorim, A., Dommen, J., Duplissy, J., Hakala, J., Hansel, A., Heinritzi, M., Kangasluoma,
1104 J., Kirkby, J., Krapf, M., Kürten, A., Lehtipalo, K., Riccobono, F., Rondo, L., Sarnela, N., Simon, M.,
1105 Tomé, A., Tröstl, J., Winkler, P. M., Williamson, C., Ye, P., Curtius, J., Baltensperger, U., Donahue, N.
1106 M., Kulmala, M., and Worsnop, D. R.: Elemental composition and clustering behaviour of α-pinene

oxidation products for different oxidation conditions, Atmos. Chem. Phys., 15, 4145-4159, doi: 10.5194/acp-15-4145-2015, 2015.

Rantala, P., Taipale, R., Aalto, J., Kajos, M. K., Patokoski, J., Ruuskanen, T. M., and Rinne, J.: Continuous flux measurements of VOCs using PTR-MS – reliability and feasibility of disjunct-eddy-covariance, surface-layer-gradient, and surface-layer-profile methods, Boreal Env. Res., 19 (suppl. B), 87–107, 2014.

Rohrer, F., and Berreheim, H.: Strong correlation between levels of tropospheric hydroxyl radicals and solar ultraviolet radiation, Nature, 442, 184–187, doi: 10.1038/nature04924, 2006.

Riccobono, F., Schobesberger, S., Scott, C. E., Dommen, J., Ortega, I. K., Rondo, L., Almeida, J., Amorim, A., Bianchi, F., Breitenlechner, M., David, A., Downard, A., Dunne, E. M., Duplissy, J., Ehrhart, S., Flagan, R. C., Franchin, A., Hansel, A., Junninen, H., Kajos, M., Keskinen, H., Kupc, A., Kürten, A., Kvashin, A. N., Laaksonen, A., Lehtipalo, K., Makhmutov, V., Mathot, S., Nieminen, T., Onnela, A., Petäjä, T., Praplan, A. P., Santos, F. D., Schallhart, S., Seinfeld, J. H., Sipilä, M., Spracklen, D. V., Stozhkov, Y., Stratmann, F., Tomé, A., Tsagkogeorgas, G., Vaattovaara, P., Viisanen, Y., Vrtala, A., Wagner, P. E., Weingartner, E., Wex, H., Wimmer, D., Carslaw, K. S., Curtius, J., Donahue, N. M., Kirkby, J., Kulmala, M., Worsnop, D. R., and Baltensperger, U.: Oxidation products of biogenic emissions contribute to nucleation of atmospheric particles, Science, 344, 717–721, doi: 10.1126/science.1243527, 2014.

Rondo, L., Kürten, A., Ehrhart, S., Schobesberger, S., Franchin, A., Junninen, H., Petäjä, T., Sipilä, M., Worsnop, D. R., and Curtius, J.: Effect of ions on the measurement of sulfuric acid in the CLOUD experiment at CERN, Atmos. Meas. Tech., 7, 3849–3859, doi: 10.5194/amt-7-3849-2014, 2014.

Saiz-Lopez, A., Plane, J. M. C., Baker, A. R., Carpenter, L. J., von Glasow, R., Martín, J. C. G., McFiggans, G., and Saunders, R. W.: Atmospheric chemistry of iodine, Chem. Rev., 112, 1773–1804, doi: 10.1021/cr200029u, 2012.

Saiz-Lopez, A., Baidar, S., Cuevas, C. A., Koenig, T. K., Fernandez, R. P., Dix, B., Kinnison, D. E., Lamarque, J.-F. , Rodriguez-Lloveras, X., Campos, T. L., and Volkamer, R.: Injection of iodine to the stratosphere, Geophys. Res. Lett., 42, 6852–6859, doi: 10.1002/2015GL064796, 2015.

Sarnela, N., Jokinen, T., Nieminen, T., Lehtipalo, K., Junninen, H., Kangasluoma, J., Hakala, J., Taipale, R., Schobesberger, S., Sipilä, M., Larnimaa, K., Westerholm, H., Heijari, J., Kerminen, V.-M., Petäjä,

1143 T., and Kulmala, M.: Sulphuric acid and aerosol particle production in the vicinity of an oil refinery,
1144 Atmos. Env., 119, 156–166, doi: 10.1016/j.atmosenv.2015.08.033, 2015.
1145
1146 Sarwar, G., Fahey, K., Kwok, R., Gilliam, R. C., Roselle, S. J., Mathur, R., Xue, J., Yu, J., and Carter,
1147 W. P. L.: Potential impacts of two SO_2 oxidation pathways on regional sulphate concentrations:
1148 Aqueous-phase oxidation by NO_2 and gas-phase oxidation by stabilized Criegee intermediate, Atmos.
1149 Env., 68, 186–197, doi: 10.1016/j.atmosenv.2012.11.036, 2013.
1150
1151 Schade, G. W., and Crutzen, P. J.: Emission of aliphatic amines from animal husbandry and their
1152 reactions: Potential source of N_2O and HCN, J. Atmos. Chem., 22, 319–346, doi: 10.1007/BF00696641,
1153 1995.
1154
1155 Schobesberger, S., Junninen, H., Bianchi, F., Lönn, G., Ehn, M., Lehtipalo, K., Dommen, J., Ehrhart,
1156 S., Ortega, I. K., Franchin, A., Nieminen, T., Riccobono, F., Hutterli, M., Duplissy, J., Almeida, J.,
1157 Amorim, A., Breitenlechner, M., Downard, A. J., Dunne, E. M., Flagan, R. C., Kajos, M., Keskinen, H.,
1158 Kirkby, J., Kupc, A., Kürten, A., Kurtén, T., Laaksonen, A., Mathot, S., Onnela, A., Praplan, A. P.,
1159 Rondo, L., Santos, F. D., Schallhart, S., Schnitzhofer, R., Sipilä, M., Tomé, A., Tsagkogeorgas, G.,
1160 Vehkamäki, H., Wimmer, D., Baltensperger, U., Carslaw, K. S., Curtius, J., Hansel, A., Petäjä, T.,
1161 Kulmala, M., Donahue, N. M., and Worsnop, D. R.: Molecular understanding of atmospheric particle
1162 formation from sulfuric acid and large oxidized organic molecules, Proc. Natl. Acad. Sci. USA, 110,
1163 17223–17228, doi: 10.1073/pnas.1306973110, 2013.
1164
1165 Sihto, S.-L., Kulmala, M., Kerminen, V.-M., Dal Maso, M., Petäjä, T., Riipinen, I., Korhonen, H.,
1166 Arnold, F., Janson, R., Boy, M., Laaksonen, A., and Lehtinen, K. E. J.: Atmospheric sulphuric acid and
1167 aerosol formation: implications from atmospheric measurements for nucleation and early growth
1168 mechanisms, Atmos. Chem. Phys., 6, 4079–4091, doi: 10.5194/acp-6-4079-2006, 2006.
1169
1170 Simon, M., Heinritzi, M., Herzog, S., Leiminger, M., Bianchi, F., Praplan, A., Dommen, J., Curtius, J.,
1171 and Kürten, A.: Detection of dimethylamine in the low pptv range using nitrate chemical ionization
1172 atmospheric pressure interface time-of-flight (CI-APi-TOF) mass spectrometry, Atmos. Meas. Tech., 9,
1173 2135-2145, doi: 10.5194/amt-9-2135-2016, 2016.
1174
1175 Sintermann, J., Schallhart, S., Kajos, M., Jocher, M., Bracher, A., Münger, A., Johnson, D., Neftel, A.,
1176 and Ruuskanen, T.: Trimethylamine emissions in animal husbandry, Biogeosciences, 11, 5073–5085,
1177 doi: 10.5194/bg-11-5073-2014, 2014.
1178

1179 Sipilä, M., Sarnela, N., Jokinen, T., Junninen, H., Hakala, J., Rissanen, M. P., Praplan, A., Simon, M.,
1180 Kürten, A., Bianchi, F., Dommen, J., Curtius, J., Petäjä, T., and Worsnop, D. R.: Bisulfate – cluster
1181 based atmospheric pressure chemical ionization mass spectrometer for high-sensitivity (< 100 ppqV)
1182 detection of atmospheric dimethyl amine: proof-of-concept and first ambient data from boreal forest,
1183 Atmos. Meas. Tech., 8, 4001–4011, doi: 10.5194/amt-8-4001-2015, 2015.
1184
1185 Stein, A. F., Draxler, R. R, Rolph, G. D., Stunder, B. J. B., Cohen, M. D., and Ngan, F.: NOAA's
1186 HYSPLIT atmospheric transport and dispersion modeling system, Bull. Amer. Meteor. Soc., 96, 2059–
1187 2077, doi: 10.1175/BAMS-D-14-00110.1, 2015.
1188
1189 Tani, A., Hayward, S., and Hewitt, C. N.: Measurement of monoterpenes and related compounds by
1190 proton transfer reaction-mass spectrometry (PTR-MS), Int. J. Mass Spectrom., 223, 561–578, doi:
1191 10.1016/S1387-3806(02)00880-1, 2003.
1192
1193 Vanhanen, J. , Mikkilä, J. , Lehtipalo, K. , Sipilä, M. , Manninen, H. E. , Siivola, E. , Petäjä, T., and
1194 Kulmala, M.: Particle size magnifier for nano-CN detection, Aerosol Sci. Technol., 45, 533–542, doi:
1195 10.1080/02786826.2010.547889, 2011.
1196
1197 von Bobrutzki, K., Braban, C. F., Famulari, D., Jones, S. K., Blackall, T., Smith, T. E. L., Blom, M.,
1198 Coe, H., Gallagher, M., Ghalaieny, M., McGillen, M. R., Percival, C. J., Whitehead, J. D., Ellis, R.,
1199 Murphy, J., Mohacsi, A., Pogany, A., Junninen, H., Rantanen, S., Sutton, M. A., and Nemitz, E.: Field
1200 inter-comparison of eleven atmospheric ammonia measurement techniques, Atmos. Meas. Tech., 3, 91–
1201 112, doi: 10.5194/amt-3-91-2010, 2010.
1202
1203 Weber, R. J., Marti, J. J., McMurry, P. H., Eisele, F. L., Tanner, D. J., and Jefferson, A.: Measurements
1204 of new particle formation and ultrafine particle growth rates at a clean continental site, J. Geophys. Res.,
1205 102, D4, 4375–4385, doi: 10.1029/96JD03656, 1997.
1206
1207 You, Y., Kanawade, V. P., de Gouw, J. A., Guenther, A. B., Madronich, S., Sierra-Hernández, M. R.,
1208 Lawler, M., Smith, J. N., Takahama, S., Ruggeri, G., Koss, A., Olson, K., Baumann, K., Weber, R. J.,
1209 Nenes, A., Guo, H., Edgerton, E. S., Porcelli, L., Brune, W. H., Goldstein, A. H., and Lee, S.-H.:
1210 Atmospheric amines and ammonia measured with a chemical ionization mass spectrometer (CIMS),
1211 Atmos. Chem. Phys., 14, 12181–12194, doi: 10.5194/acp-14-12181-2014, 2014.
1212
1213 Yu, H., and Lee, S.-H.: Chemical ionisation mass spectrometry for the measurement of atmospheric
1214 amines, Env. Chem., 9, 190–201, doi: 10.1071/EN12020, 2012.
1215

1216 Zhang, R., Khalizov, A., Wang, L., Hu, M., and Xu, W.: Nucleation and growth of nanoparticles in the
1217 atmosphere, Chem. Rev., 1957–2011, doi: 10.1021/cr2001756, 2012.
1218
1219 Zhao, J., Eisele, F. L., Titcombe, M., Kuang, C., and McMurry, P. H.: Chemical ionization mass
1220 spectrometric measurements of atmospheric neutral clusters using the cluster-CIMS, J. Geophys. Res.,
1221 115, D08205, doi: 10.1029/2009JD012606, 2010.
1222
1223 Zhao, J., Smith, J. N., Eisele, F. L., Chen, M., Kuang, C., and McMurry, P. H.: Observation of neutral
1224 sulfuric acid-amine containing clusters in laboratory and ambient measurements, Atmos. Chem. Phys.,
1225 11, 10823–10836, doi: 10.5194/acp-11-10823-2011, 2011.
1226
1227 Zhao, J., Ortega, J., Chen, M., McMurry, P. H., and Smith, J. N.: Dependence of particle nucleation and
1228 growth on high-molecular-weight gas-phase products during ozonolysis of α-pinene, Atmos. Chem.
1229 Phys., 13, 7631–7644, doi: 10.5194/acp-13-7631-2013, 2013.

Atmos. Chem. Phys. Discuss., doi:10.5194/acp-2016-294, 2016
Manuscript under review for journal Atmos. Chem. Phys.
Published: 6 June 2016

Atmospheric Chemistry and Physics Discussions

Table 1. List of ions used in the identification of sulfuric acid (monomer and dimer), iodic acid, ammonia, amines (C1, C2, C3, C4 and C6) and dimethylnitrosamine. Cattle farms in the vicinity of the measurement site are expected to be a source for the listed amines (Ge et al., 2011).

Ion	Exact mass	Neutral compound
HSO_4^-, $(HNO_3)HSO_4^-$	96.9601, 159.9557	sulfuric acid monomer
$(H_2SO_4)HSO_4^-$, $(HNO_3)(H_2SO_4)HSO_4^-$	194.9275, 257.9231	sulfuric acid dimer
IO_3^-, $(H_2O)IO_3^-$, $(HNO_3)IO_3^-$	174.8898, 192.9003, 237.8854	iodic acid
$(NH_3)(HNO_3)_{1,2}NO_3^-$	142.0106, 205.0062	ammonia
$(CH_5N)(HNO_3)_{1,2}NO_3^-$	156.0262, 219.0219	C1-amines (e.g. methylamine)
$(C_2H_7N)(HNO_3)_{1,2}NO_3^-$	170.0419, 233.0375	C2-amines (e.g. ethylamine, dimethylamine)
$(C_3H_9N)(HNO_3)_{1,2}NO_3^-$	184.0575, 247.0532	C3-amines (e.g. trimethylamine, propylamine)
$(C_4H_{11}N)(HNO_3)_{1,2}NO_3^-$	198.0732, 261.0688	C4-amines (e.g. diethylamine, butylamine)
$(C_6H_{15}N)(HNO_3)_{1,2}NO_3^-$	226.1045, 289.1001	C6-amines (e.g. triethylamine)
$(C_2H_6N_2O)(HNO_3)_{1,2}NO_3^-$	199.0320, 262.0277	dimethylnitrosamine

Atmos. Chem. Phys. Discuss., doi:10.5194/acp-2016-294, 2016
Manuscript under review for journal Atmos. Chem. Phys.
Published: 6 June 2016

Atmospheric Chemistry and Physics Discussions

Table 2. Peak list of the highly oxidized organic molecules (HOM) used in this study.

Ion sum formula	Cluster ion	Exact mass	Compound
$C_{10}H_{15}NO_9^-$	$(C_{10}H_{15}O_6)NO_3^-$	293.0752	HOM RO_2 radical
$C_{10}H_{15}NO_{10}^-$	$(C_{10}H_{15}O_7)NO_3^-$	309.0701	HOM RO_2 radical
$C_{10}H_{15}NO_{11}^-$	$(C_{10}H_{15}O_8)NO_3^-$	325.0651	HOM RO_2 radical
$C_{10}H_{15}NO_{12}^-$	$(C_{10}H_{15}O_9)NO_3^-$	341.0600	HOM RO_2 radical
$C_{10}H_{15}NO_{13}^-$	$(C_{10}H_{15}O_{10})NO_3^-$	357.0549	HOM RO_2 radical
$C_{10}H_{15}NO_{15}^-$	$(C_{10}H_{15}O_{12})NO_3^-$	389.0447	HOM RO_2 radical
$C_8H_{12}NO_{11}^-$	$(C_8H_{12}O_8)NO_3^-$	298.0416	HOM monomer
$C_9H_{14}NO_{12}^-$	$(C_9H_{14}O_9)NO_3^-$	328.0521	HOM monomer
$C_{10}H_{14}NO_{10}^-$	$(C_{10}H_{14}O_7)NO_3^-$	308.0623	HOM monomer
$C_{10}H_{14}NO_{11}^-$	$(C_{10}H_{14}O_8)NO_3^-$	324.0572	HOM monomer
$C_{10}H_{14}NO_{12}^-$	$(C_{10}H_{14}O_9)NO_3^-$	340.0521	HOM monomer
$C_{10}H_{14}NO_{13}^-$	$(C_{10}H_{14}O_{10})NO_3^-$	356.0471	HOM monomer
$C_{10}H_{14}NO_{14}^-$	$(C_{10}H_{14}O_{11})NO_3^-$	372.0420	HOM monomer
$C_{10}H_{16}NO_9^-$	$(C_{10}H_{16}O_6)NO_3^-$	294.0831	HOM monomer
$C_{10}H_{16}NO_{10}^-$	$(C_{10}H_{16}O_7)NO_3^-$	310.0780	HOM monomer
$C_{10}H_{16}NO_{11}^-$	$(C_{10}H_{16}O_8)NO_3^-$	326.0729	HOM monomer
$C_{10}H_{16}NO_{12}^-$	$(C_{10}H_{16}O_9)NO_3^-$	342.0678	HOM monomer
$C_{10}H_{16}NO_{13}^-$	$(C_{10}H_{16}O_{10})NO_3^-$	358.0627	HOM monomer
$C_{10}H_{16}NO_{14}^-$	$(C_{10}H_{16}O_{11})NO_3^-$	374.0576	HOM monomer
$C_{10}H_{15}N_2O_{10}^-$	$(C_{10}H_{15}NO_7)NO_3^-$	323.0732	HOM nitrate
$C_{10}H_{15}N_2O_{11}^-$	$(C_{10}H_{15}NO_8)NO_3^-$	339.0681	HOM nitrate
$C_{10}H_{15}N_2O_{12}^-$	$(C_{10}H_{15}NO_9)NO_3^-$	355.0630	HOM nitrate
$C_{10}H_{15}N_2O_{13}^-$	$(C_{10}H_{15}NO_{10})NO_3^-$	371.0580	HOM nitrate
$C_{10}H_{15}N_2O_{14}^-$	$(C_{10}H_{15}NO_{11})NO_3^-$	387.0529	HOM nitrate
$C_{10}H_{15}N_2O_{15}^-$	$(C_{10}H_{15}NO_{12})NO_3^-$	403.0478	HOM nitrate
$C_{10}H_{15}N_2O_{16}^-$	$(C_{10}H_{15}NO_{13})NO_3^-$	419.0427	HOM nitrate
$C_{10}H_{16}N_3O_{11}^-$	$(C_{10}H_{16}N_2O_8)NO_3^-$	354.0790	HOM di-nitrate
$C_{10}H_{17}N_4O_{14}^-$	$(C_{10}H_{16}N_2O_8)(HNO_3)NO_3^-$	417.0747	HOM di-nitrate
$C_{10}H_{16}N_3O_{12}^-$	$(C_{10}H_{16}N_2O_9)NO_3^-$	370.0739	HOM di-nitrate
$C_{10}H_{17}N_4O_{15}^-$	$(C_{10}H_{16}N_2O_9)(HNO_3)NO_3^-$	433.0696	HOM di-nitrate
$C_{10}H_{16}N_3O_{13}^-$	$(C_{10}H_{16}N_2O_{10})NO_3^-$	386.0689	HOM di-nitrate
$C_{10}H_{17}N_4O_{16}^-$	$(C_{10}H_{16}N_2O_{10})(HNO_3)NO_3^-$	449.0645	HOM di-nitrate
$C_{19}H_{30}NO_{16}^-$	$(C_{19}H_{30}O_{13})NO_3^-$	528.1570	HOM dimer
$C_{19}H_{30}NO_{17}^-$	$(C_{19}H_{30}O_{14})NO_3^-$	544.1519	HOM dimer
$C_{20}H_{28}NO_{16}^-$	$(C_{20}H_{28}O_{13})NO_3^-$	538.1414	HOM dimer
$C_{20}H_{28}NO_{17}^-$	$(C_{20}H_{28}O_{14})NO_3^-$	554.1363	HOM dimer
$C_{20}H_{28}NO_{18}^-$	$(C_{20}H_{28}O_{15})NO_3^-$	570.1312	HOM dimer
$C_{20}H_{28}NO_{19}^-$	$(C_{20}H_{28}O_{16})NO_3^-$	586.1261	HOM dimer
$C_{20}H_{28}NO_{20}^-$	$(C_{20}H_{28}O_{17})NO_3^-$	602.1210	HOM dimer
$C_{20}H_{28}NO_{21}^-$	$(C_{20}H_{28}O_{18})NO_3^-$	618.1159	HOM dimer
$C_{20}H_{28}NO_{22}^-$	$(C_{20}H_{28}O_{19})NO_3^-$	634.1108	HOM dimer
$C_{20}H_{28}NO_{23}^-$	$(C_{20}H_{28}O_{20})NO_3^-$	650.1058	HOM dimer
$C_{20}H_{30}NO_{17}^-$	$(C_{20}H_{30}O_{14})NO_3^-$	556.1519	HOM dimer

Atmos. Chem. Phys. Discuss., doi:10.5194/acp-2016-294, 2016
Manuscript under review for journal Atmos. Chem. Phys.
Published: 6 June 2016

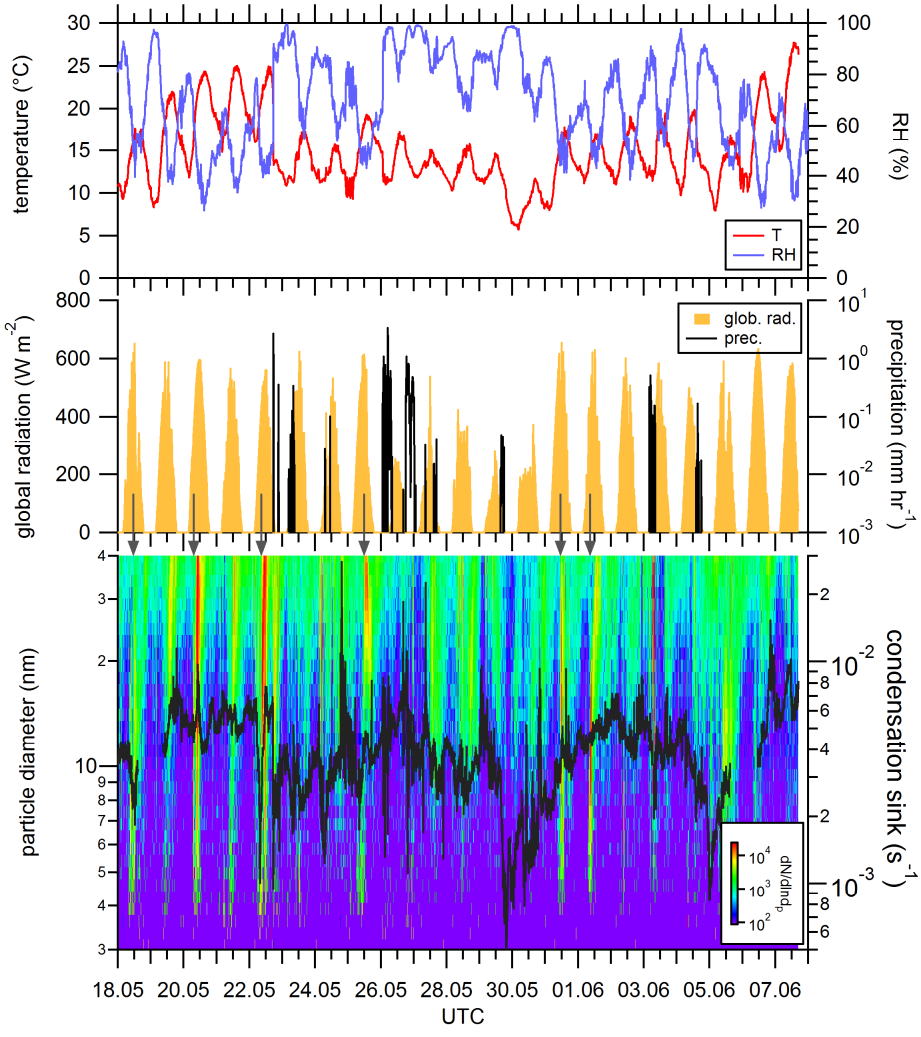

Fig. 1. Overview of the different parameters measured between May 18 and June 8, 2014. Temperature (T) and relative humidity (RH) are shown in the upper panel, the center panel shows the global radiation and precipitation, while the bottom panel shows the number size distribution measured by the nano-DMA together with the condensation sink (black line).

Atmos. Chem. Phys. Discuss., doi:10.5194/acp-2016-294, 2016
Manuscript under review for journal Atmos. Chem. Phys.
Published: 6 June 2016

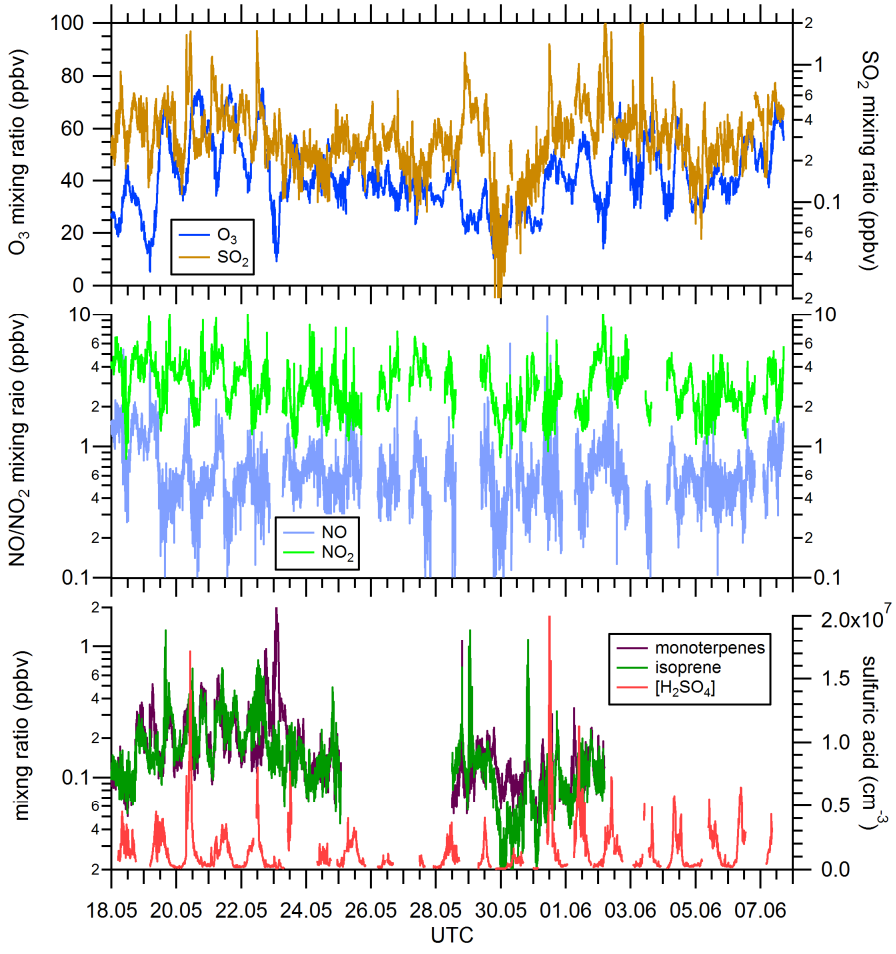

Fig. 2. Overview of the trace gas measurements between May 18 and June 8, 2014. The SO_2 and O_3 mixing ratios are shown in the upper panel, the NO and NO_2 mixing ratio are shown in the center panel and the bottom panel shows the sulfuric acid monomer concentration ($[H_2SO_4]$) together with the isoprene and monoterpene mixing ratios.

Atmos. Chem. Phys. Discuss., doi:10.5194/acp-2016-294, 2016
Manuscript under review for journal Atmos. Chem. Phys.
Published: 6 June 2016

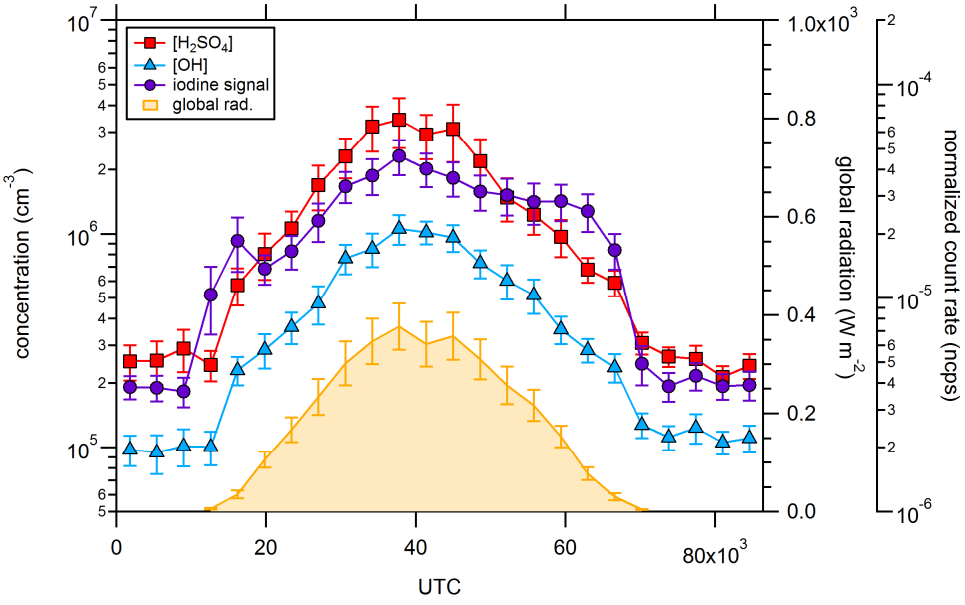

Fig. 3. Diurnal averages for the sulfuric acid ($[H_2SO_4]$) and the calculated hydroxyl radical ([OH]) concentrations (axis on the left). The iodine signal is not converted into a concentration, instead the normalized count rates per second (ncps) are shown (axis on the right). A value of 5×10^{-5} ncps for iodine would correspond to a concentration of 3×10^{5} molecule cm^{-3} applying the same conversion factor for iodic acid than for sulfuric acid. The global radiation indicates that all signals are related to photochemistry. Error bars indicate one standard deviation for the 30-minute averaged values.

Atmos. Chem. Phys. Discuss., doi:10.5194/acp-2016-294, 2016
Manuscript under review for journal Atmos. Chem. Phys.
Published: 6 June 2016

Atmospheric Chemistry and Physics Discussions

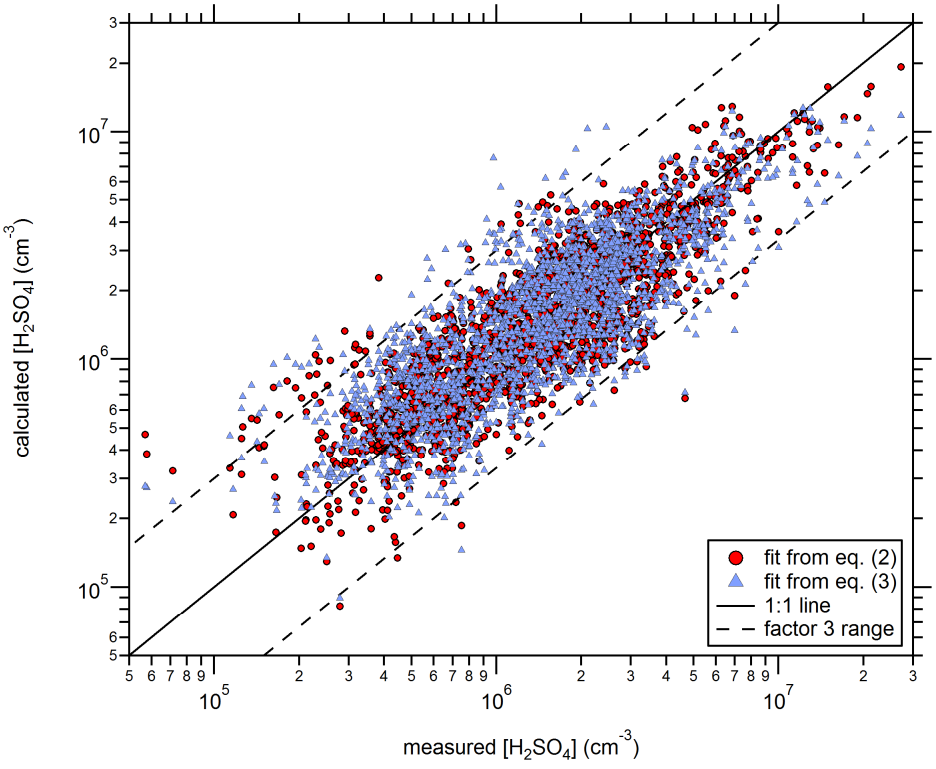

Fig. 4. Calculated [H_2SO_4] as a function of the measured concentrations. Only data points where the global radiation exceeded 50 W m^{-2} were considered in deriving the fit parameters for equations (2) and (3). The red circles take into account SO_2, global radiation (*Rad*), condensation sink (*CS*) and relative humidity (RH) to calculate the [H_2SO_4], whereas only SO_2 and global radiation are used for the blue triangles.

Atmos. Chem. Phys. Discuss., doi:10.5194/acp-2016-294, 2016
Manuscript under review for journal Atmos. Chem. Phys.
Published: 6 June 2016

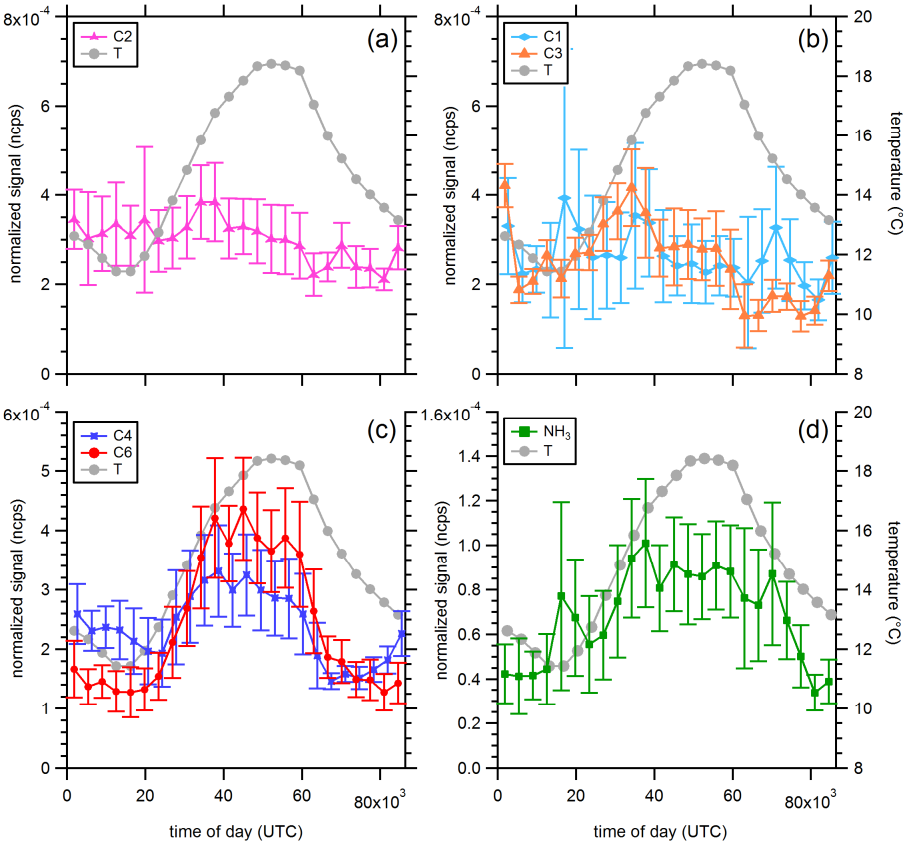

Fig. 5. Diurnal averages for different amines (C1, C2, C3, C4 and C6) and ammonia. The temperature profile is shown in addition. Error bars represent one standard deviation of the 30-minute averages. The lower detection limits for the different compounds are not well-defined, however, the lowest measured signals during some periods were 0.3×10^{-4} ncps for C1, ~0.5×10^{-4} ncps for C2, C3, C4 and C6 and 0.1×10^{-4} ncps for ammonia. For most of the time (and for all averaged values shown) the signals were clearly above these "background" levels.

Atmos. Chem. Phys. Discuss., doi:10.5194/acp-2016-294, 2016
Manuscript under review for journal Atmos. Chem. Phys.
Published: 6 June 2016

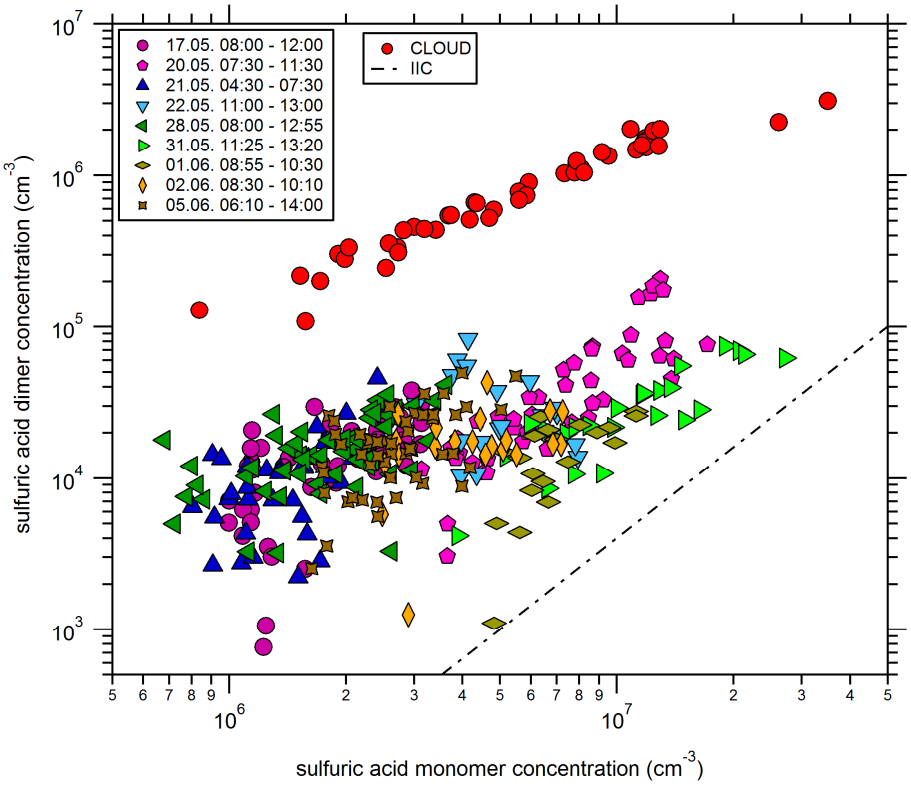

Fig. 6. Sulfuric acid dimer concentrations as a function of the sulfuric acid monomer concentrations. The legend on the left lists the periods when high dimer signals were observed. In addition, data from CLOUD chamber experiments with at least 10 pptv of dimethylamine are shown; under these conditions dimer formation proceeds at or close to the kinetic limit (Kürten et al., 2014). The dashed-dotted line indicates the lower detection limit for neutral dimers set by ion induced clustering (IIC) within the CI-APi-TOF ion reaction zone.

Atmos. Chem. Phys. Discuss., doi:10.5194/acp-2016-294, 2016
Manuscript under review for journal Atmos. Chem. Phys.
Published: 6 June 2016

Atmospheric Chemistry and Physics Discussions

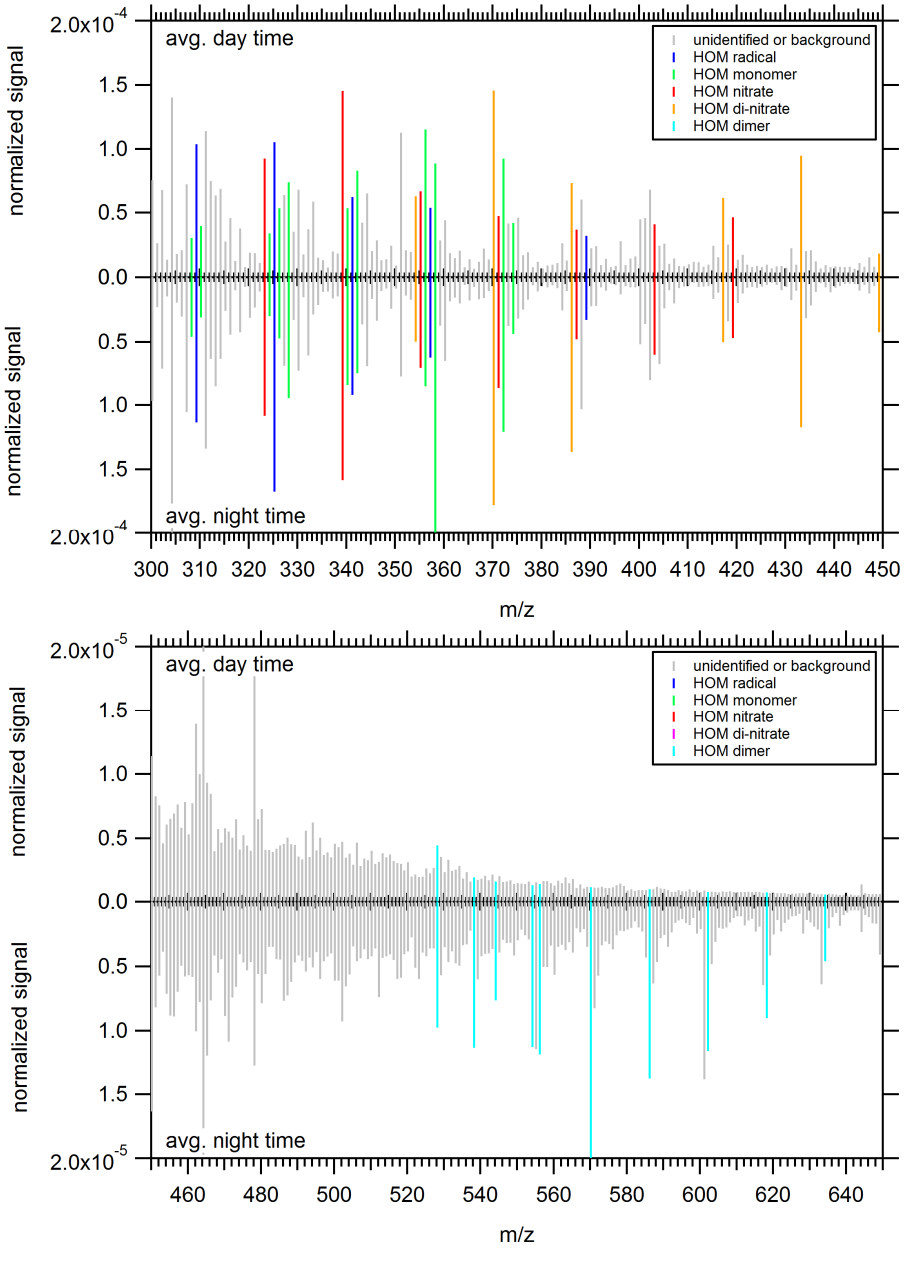

1275

1276 **Fig. 7.** Comparison between average day time and night time mass spectra measured with the nitrate CI-

1277 APi-TOF. The day time spectrum was averaged for periods when no nucleation was observed.

Atmos. Chem. Phys. Discuss., doi:10.5194/acp-2016-294, 2016
Manuscript under review for journal Atmos. Chem. Phys.
Published: 6 June 2016

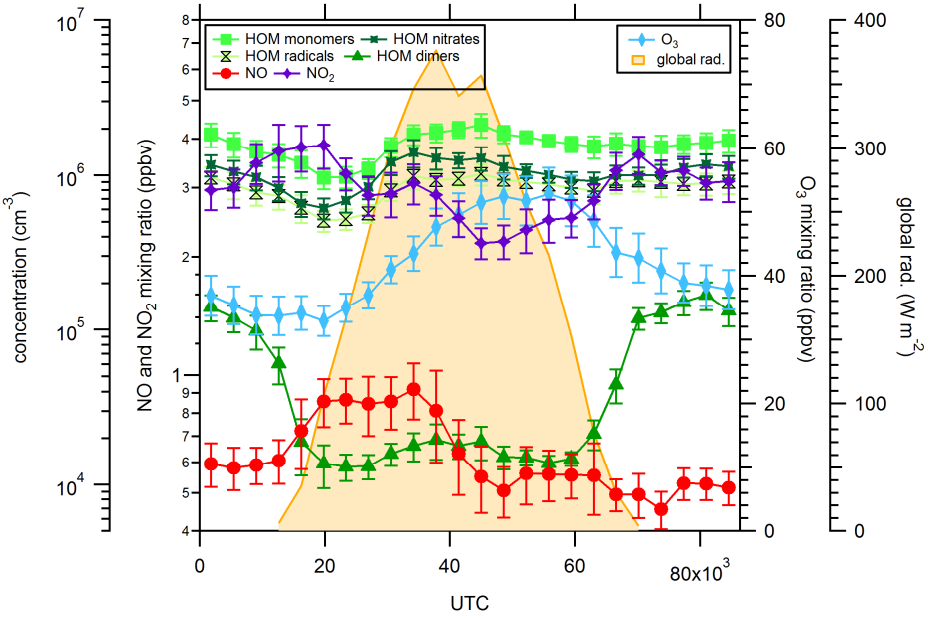

Fig. 8. Diurnal profiles of the NO, NO_2 and O_3 mixing ratios. The signals for highly oxidized organic molecules (HOM) are shown for some C10 (HOM monomers, HOM nitrates and HOM radicals) and C19/C20 compounds (HOM dimers), which show a distinct maximum during the night. The HOM di-nitrates show a similar pattern as the other C10 compounds and are not included in the figure. The global radiation is shown in addition. Error bars indicate one standard deviation for the 30-minute averages.

Atmos. Chem. Phys. Discuss., doi:10.5194/acp-2016-294, 2016
Manuscript under review for journal Atmos. Chem. Phys.
Published: 6 June 2016

Atmospheric Chemistry and Physics Discussions

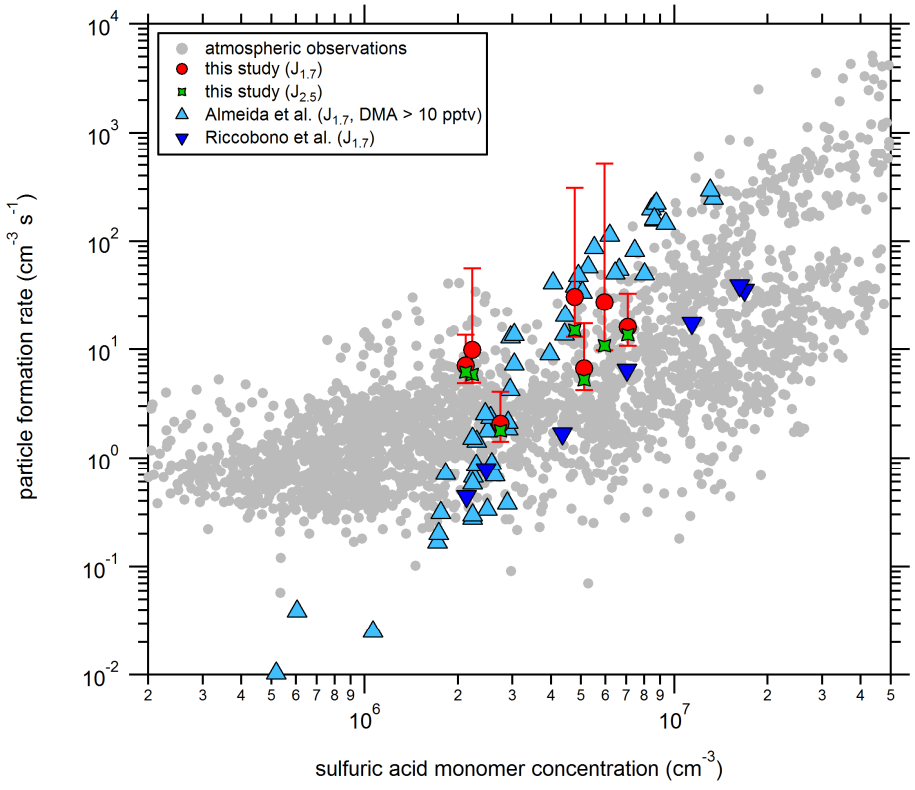

Fig. 9. Particle formation rates form this study at a mobility diameter of 1.7 nm ($J_{1.7}$ red circles) and 2.5 nm ($J_{2.5}$, green stars). Data from CLOUD chamber measurements for a diameter of 1.7 nm are shown in addition for the system of sulfuric acid, water and dimethylamine (light blue symbols, see Almeida et al., 2013) and sulfuric acid, water and oxidized organics from pinanediol (dark blue symbols, see Riccobono et al., 2014). The light grey circles are from other field measurements (Kuang et al., 2008; Paasonen et al., 2010; Kulmala et al., 2013).

Atmos. Chem. Phys. Discuss., doi:10.5194/acp-2016-294, 2016
Manuscript under review for journal Atmos. Chem. Phys.
Published: 6 June 2016

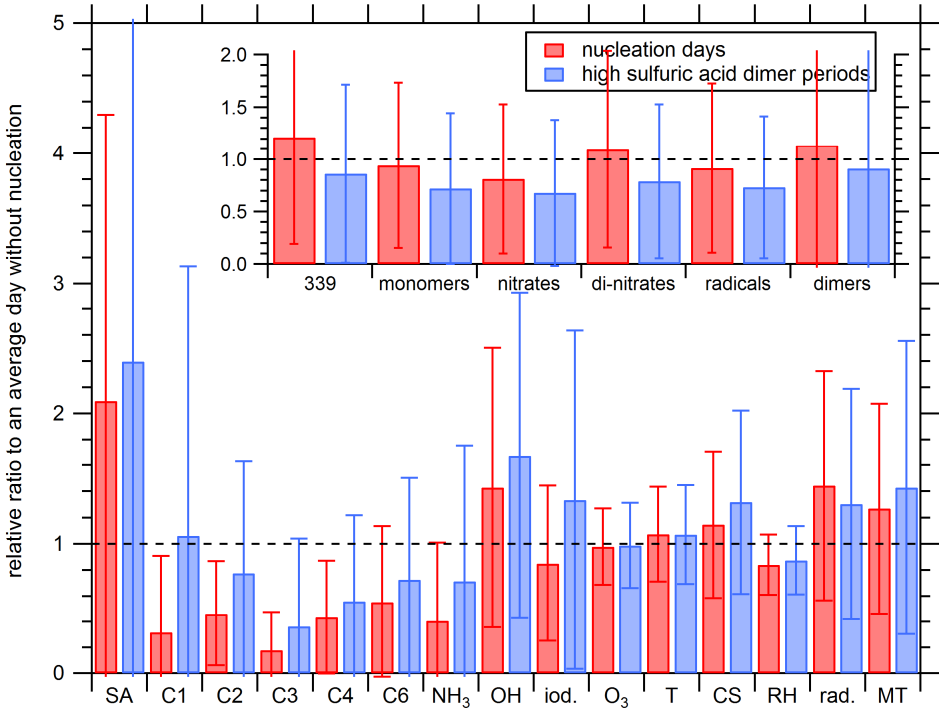

Fig. 10. Comparison of various parameters for different time periods (SA = sulfuric acid monomer, C1, C2, C3, C4 and C6 = amines, iod. = iodic acid and rad. = global radiation intensity). The subset figure on the upper right shows the signals for the highly oxidized organic compounds with 10 or 20 carbon atoms (339 = organic compound $C_{10}H_{15}NO_8$ clustered with NO_3^- having a mass of 339.0681 Th, the definition of other HOM, i.e. monomers, radicals, nitrates, di-nitrates and dimers can be found in Table 2). The red bars relate nucleation days to days without nucleation and the blue bars show the ratio between periods where high sulfuric acid dimer concentrations were observed (see Fig. 6) to no nucleation days. Similar times of the day (early morning) were used as reference periods when no nucleation was observed as nucleation and dimer formation was also mainly observed in the morning.